2003 Field Monitoring Report – Waves, Currents, and Sediment Transport at North Jetty

Evaluation of Dredged Sediment Re-handling: Mouth of Columbia River, North Jetty

PACIFIC
INTERNATIONAL
ENGINEERING PLLC

2003 Field Monitoring Report – Waves, Currents, and Sediment Transport at North Jetty

Evaluation of Dredged Sediment Re-handling: Mouth of Columbia River, North Jetty

Prepared by:

Philip Osborne, M.Sc., Ph.D.

October, 2003

PACIFIC INTERNATIONAL ENGINEERING PLLC
POST OFFICE BOX 1599 • 123 SECOND AVENUE SOUTH • EDMONDS, WASHINGTON • 98020

Table of Contents

Appendices

List of Figures

List of Tables

1. Introduction

Pacific International Engineering, PLLC at the request of, and in coordination with Pacific County and the Coastal Communities of Southwest Washington is evaluating alternatives that will assist the County and the US Army Engineer District, Portland, to develop and implement a new strategy for the Corps of Engineers dredging and dredged material disposal at the Mouth of Columbia River (MCR). The alternatives seek to optimize use of the dredged material for the nourishment of the littoral system of the Washington Coast to the north of MCR. The technical approach of the project will be consistent with and meet the standards of the US Army Corps of Engineers Regional Sediment Management Strategy (RSM) in providing information that assists coastal management to make effective use of littoral (and estuarine) sediment resources in an environmentally sound and economic manner over a broad scale.

An earlier phase of the project identified the technical feasibility of pumping sediment from a hopper dredge across the north jetty onto Benson Beach where it could provide a benefit by returning sediment directly to the littoral system and also offer protection to the north side of the north jetty which has become more vulnerable to wave attack as a result of erosion of Peacock Spit. A modification to this approach involves development of a sump in the north jetty area into which hopper dredges could efficiently dispose of sediment, while at other times a pipeline dredge could be used to clear the sump and re-handle the sediment to place it in the surf zone on Benson Beach. Environmental permitting considerations and exposed ocean conditions restrict dredging and disposal operations to summer months (approximately mid June through September).

As part of this evaluation, Pacific International Engineering, PLLC has collected field measurements of waves and currents in the vicinity of the north jetty during the dredging season. The measurements will provide essential data to assist in the evaluation of the potential constraints, effects, and impacts of waves and currents on pipeline dredge operations in this area, and the potential for disruption and disequilibrium of the tidal hydraulics and sediment dynamics by dredging the sump. A second objective of the measurements is to provide information to verify waves, current, and transport numerical models, thereby advancing their value as design tools to aid in the evaluation of alternatives.

This report provides a description and analysis of the coastal processes in the vicinity of the north jetty at MCR based on the recent field measurement program.

2. Field Measurement Program Overview

Field measurements of waves, currents and sediment transport are needed to characterize the wave and current climate in the proposed dredged material re-handling area and to determine the technical feasibility of a dredged sediment re-handling operation. Direct measurements of the interactions and relative importance of hydraulic forcing mechanisms and coastal processes in the dredged

material re-handling area provide the data required for calibration and verification of circulation models and a sediment transport model of the area.

A field program was conducted between July and September 2003 to collect measurements of waves, tides, currents, and sediment transport in the vicinity of the proposed dredged sediment re-handling area on the south side of north jetty at MCR. The objectives of the field measurement program are as follows:

- characterize the spatial and temporal variation of wind-, wave- and tide-induced currents in the area during the summer months (the period in which the sediment rehandling operation would be active);
- characterize the wave climate in the proposed project area by direct measurements of directional wave spectra (amplitude, frequency direction distributions); only limited data are available from previous deployments for verification of 2D wave models; a number of uncertainties arise in predicting wave heights in the MCR area based on offshore wave measurements (such as CDIP buoy) because of steep bathymetry gradients, presence of the jetties, and river-tide interactions with incoming waves;
- characterize the potential sediment transport conditions during the dredging season in the proposed sump area by measurement and analysis of the near bottom velocity field induced by combined waves and currents.

The 2003 field program consisted of the following components:

1. Point measurements of directional waves, currents and near bottom sediment transport;
2. Roving current transect measurements near north jetty combined with hydrographic survey of bathymetry.

3. Point Measurements of Waves, Currents, and Sediment Transport

Point measurements of waves, currents and near bottom sediment transport were acquired at three stations on the south side of north jetty between 25 July and 18 September 2003. The instruments were recovered and re-deployed on 21 August 2003 to service the instruments and download data. Wave data were also recorded at the National Data Buoy Center directional wave buoy (46029), operated by the National Oceanic and Atmospheric Administration (NOAA), and located approximately 18 nautical miles from north jetty in a water depth of 128 m (420 ft).

Figure 1 shows the location of the point measurement stations in relation to the north jetty and MCR. Station coordinates are given in Table 1. Station 1 was at the same location as the north jetty wave measurement station in 2002 and 2000 (PI Engineering, 2003). All stations were equipped with SonTek Hydra directional wave gauge consisting of Acoustic Doppler Velocimeter (ADV), high resolution pressure transducer (Druck or Paros), and two D & A Instruments

Optical Backscatterance Sensors (OBS-3). Stations 1 and 3 also had a SonTek Acoustic Doppler Profiler (ADP) for measurement of current profiles. Station 2 was equipped with an RD Instruments Acoustic Doppler Current Profiler (ADCP) for measurement of directional waves and current profiles. Table 2 is a summary of the instruments deployed and the sampling protocol for each station. Figures 2 through 5 show the configuration of instruments on each of the stations.

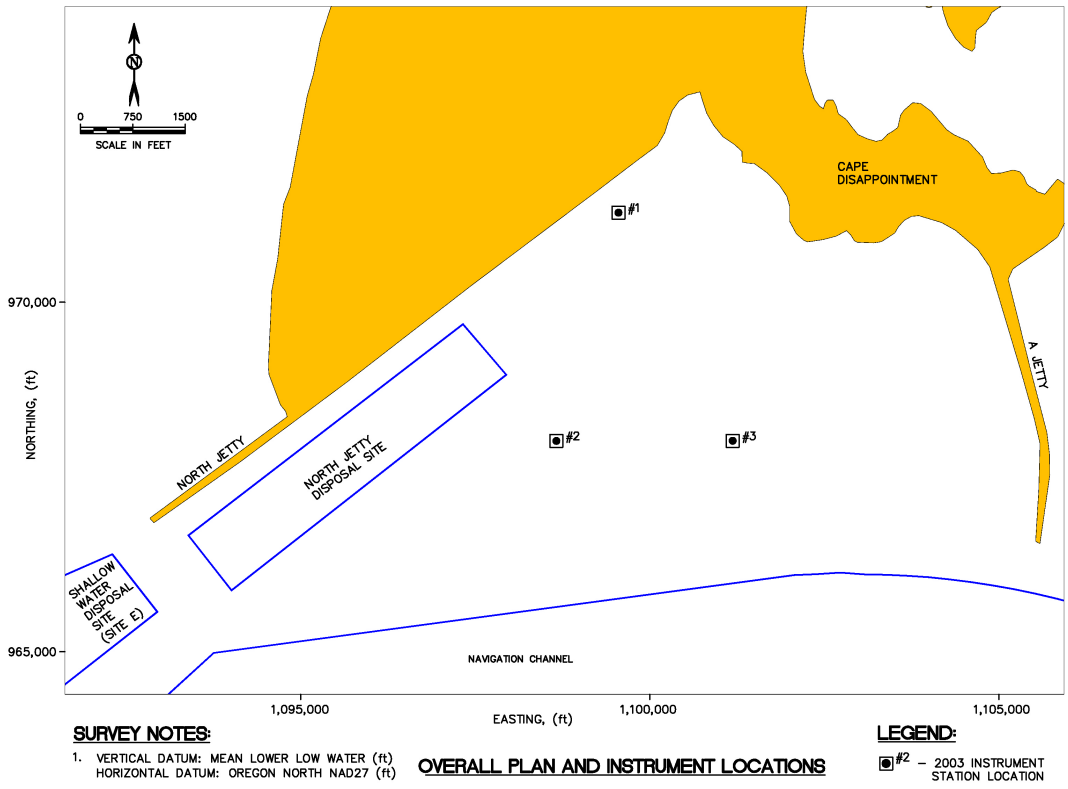

Figure 1 Location of Instrument Deployment in 2003

Table 1 Tripod Deployment and Retrieval Locations

Station ID	Deployment Date	Position				Time UTC	Elevation[3]	Retrieval Date
		Latitude[1]	Longitude[1]	Easting[2]	Northing[2]			
1	07/25/03	N46°16' 31.6"	W124°03' 6.8"	1099502	971063		-30	08/21/03
2	07/25/03	N46°16' 01.8"	W124°03' 54.5"	1098826	968077		-30	
3	07/25/03	N46°16' 02.1"	W124°03' 17.4"	1101433	967992		-30	
[1] Referred to North American Datum of 1983 – WGS84.								
[1] Referred to North American Datum of 1927 – Oregon North (in feet).								
[2] In feet referred to mean lower low water (mllw).								

Table 2 Instruments and Sampling

Station	Instrument	Data Type	Burst Interval (sec)	Burst Duration (sec)	Sampling Frequency (Hz)	Samples per Burst
1	SonTek Hydra Druck ADVO OBS-3	Directional waves/Depth 3D Velocity SSC	3600	2048	4	8192
	SonTek ADP Paros	Non-Directional waves/Depth 3D Velocity profile	3600 600	2048 180	2 1,500,000	4096
2	SonTek Hydra Paros ADVO OBS-3	Directional waves/Depth 3D Velocity SSC	3600	2048	4	8192
	RD Instruments ADCP	Directional waves/Depth 3D Velocity Profile	3600 360	1200	2 600,000	2400 180
3	SonTek Hydra Paros ADVO OBS-3	Directional waves/Depth 3D Velocity SSC	3600	2048	4	8192
	SonTek ADP Druck	Non-Directional waves/Depth 3D Velocity profile	3600 600	2048 180	2 1,500,000	4096

3.1. Data Processing and Quality Checks

A visual data quality check was performed on raw Hydra data using Sontek ViewHydra software. Data were extracted from raw data files using SonTek Hydra extraction software and written to ASCII time series, header and control files. All remaining processing and post-processing was accomplished using in-house PI Engineering software following standard analytical procedure for calculating directional wave parameters (e.g. Earle et al., 1995).

Optical backscatterance sensors (OBS-3) deployed with the Hydra systems were calibrated for suspended sediment concentration using coefficients determined in the laboratory. OBS-3 signals are recorded by the Hydra system in "counts" ranging from 100 to 65,000, which must be converted to the desired units during post processing. Calibrations were performed in a turbidity chamber following the specifications recommended by the manufacturer. Instrument gains were set prior to deployment using tap water (minimum) and 800 ntu Formazin standard solution (maximum). OBS-3 deployed were calibrated over a range of 0 to 24 g/l range at five concentrations (2 g/l, 4 g/l, 8 g/l, 16 g/l and 24 g/l) with sediment from a grab sample obtained near Station 1.

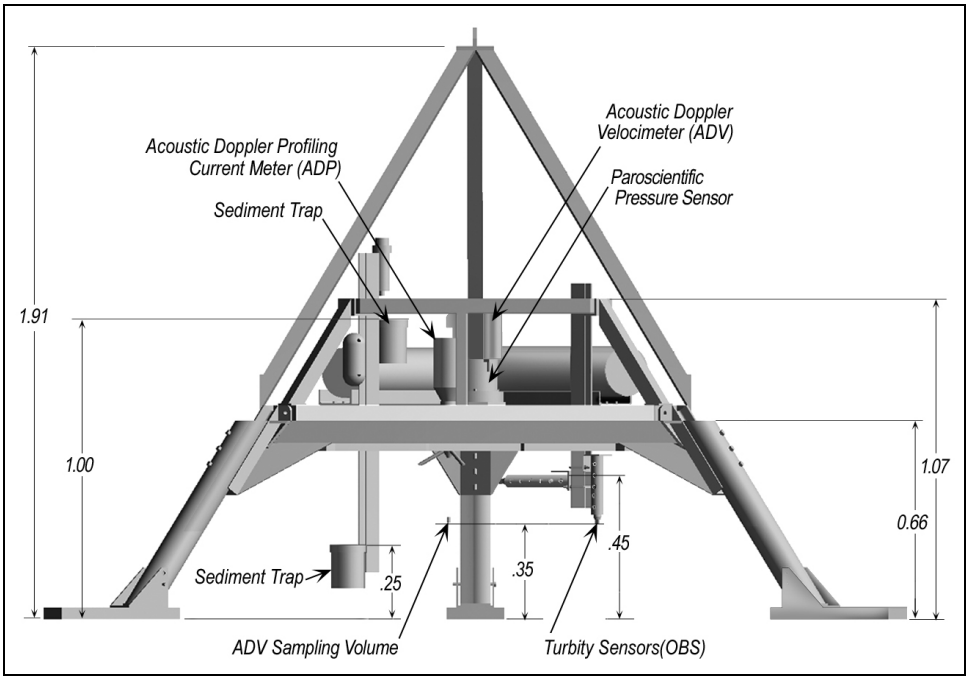

Figure 2 Tripod instrument configuration and nominal dimensions

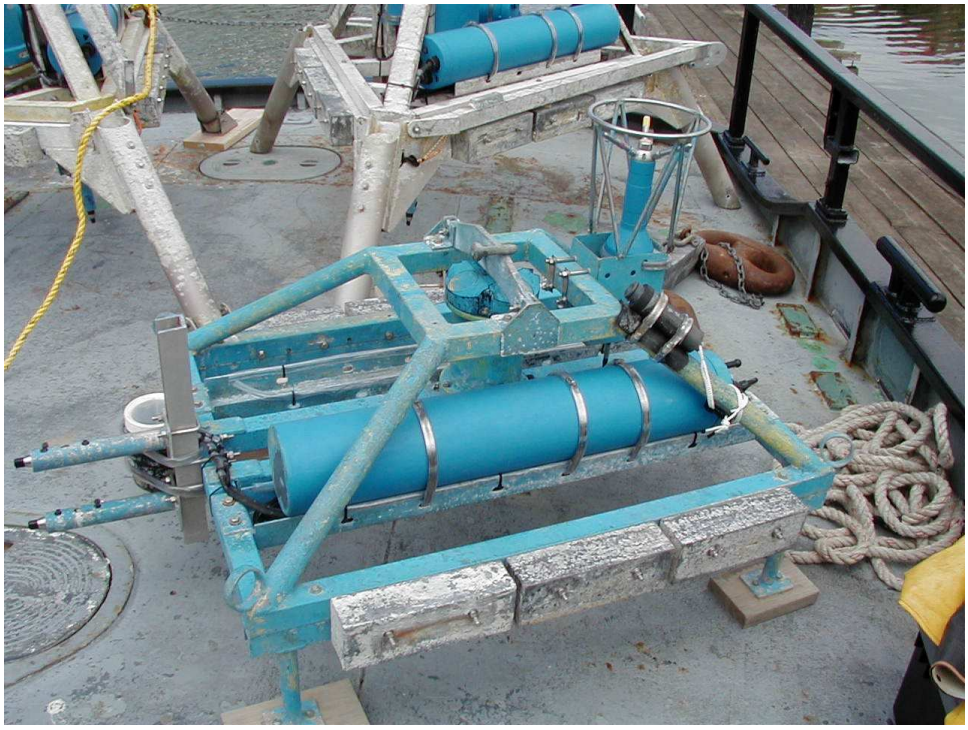

Figure 3 Wave and current monitoring Station 1

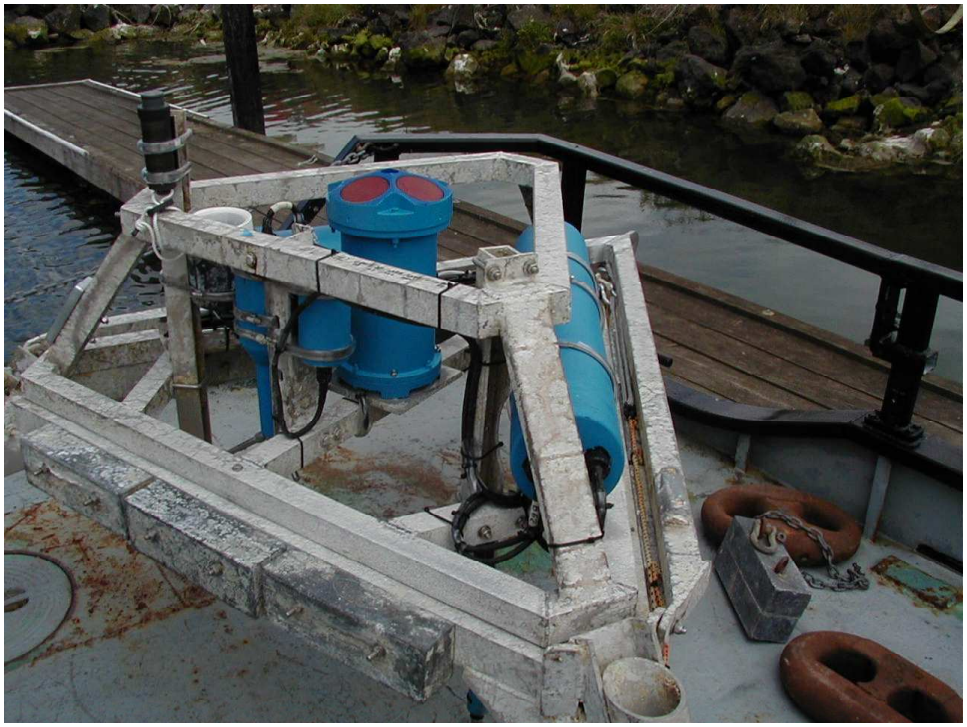

Figure 4 Wave and current monitoring Station 2

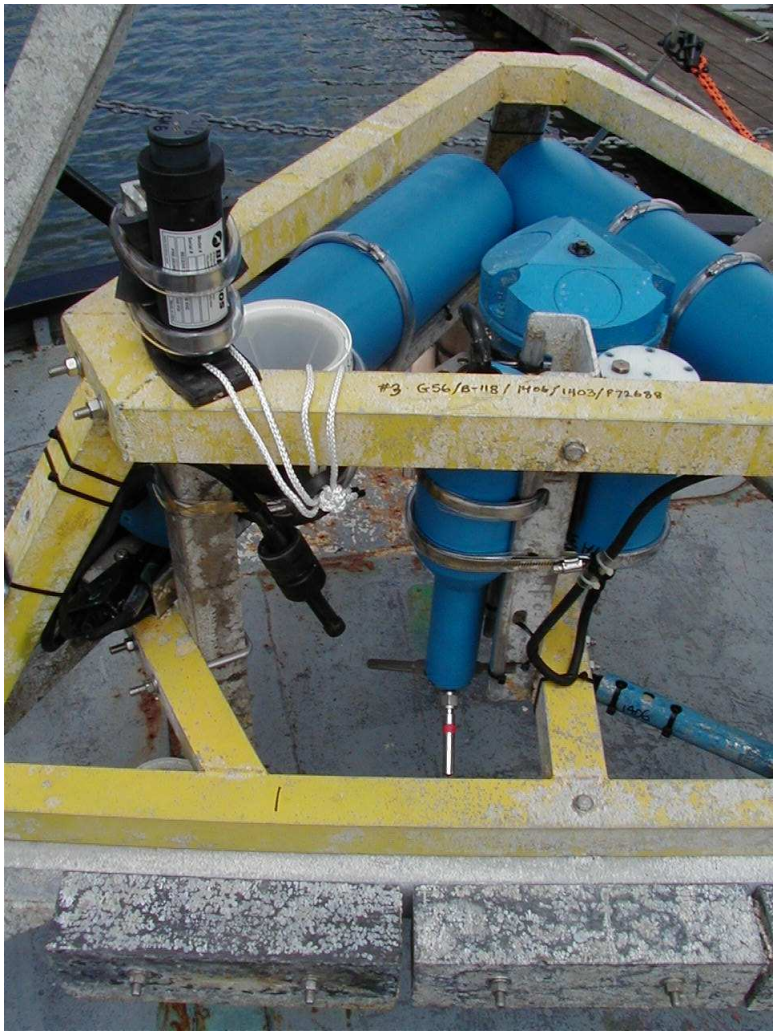

Figure 5 Wave and current monitoring Station 3

3.2. Roving Current Transect Measurements and Bathymetry Survey

Currents were measured along transects from a moving vessel to characterize the spatial variation in circulation south of north jetty during flood and ebb tides on August 12 and 13, 2003. Eight transects of 600 m to 1500 m in length were run between the north jetty and the navigation channel (Figure 6). Current and depth data were collected on two separate data acquisition systems, each with simultaneous position and time input from a single Differential Global Positioning System (DGPS) receiver. Typically, one series of eight transects was collected in 1.5 hours. Nine series of transects were collected over a 30-hour period. The transects were collected over a low tide to low tide on 2 consecutive days.

Current transect data were initially processed with ADP manufacturer's software to correct for vessel movement using ADP bottom track or DGPS-derived vessel velocity. Data quality filtering was performed to remove velocity measurements with low signal-to-noise ratios. The resultant speed and direction data were horizontally smoothed using a 5 or

7-point Gaussian filter (profile averaging) and vertically smoothed using a 3-point Gaussian filter (cell averaging). This filtering helps to minimize some of the uncorrected high-frequency velocity error resulting from vessel heave, pitch, roll and rapid turning. Depths measured simultaneously with current data were corrected using a water surface elevation time series to produce bottom elevations referenced to datum. Spikes in depth data and noise in the digital depth data were cross-referenced to paper echosounder records and erroneous data were either smoothed or deleted. Current profile speed and direction were merged with bottom elevation data to produce cross-sectional plots of speed and direction relative to distance along the planned transect line.

Vertical speed profiles were depth-averaged from 1 m below the water surface to 0.5m above bottom. Current direction was first multiplied by the current speed and then averaged to obtain a speed-weighted depth-averaged current direction. Depth-averaged speed and direction vectors were then scaled and plotted as plan-view vectors overlaid on a chart of the study area.

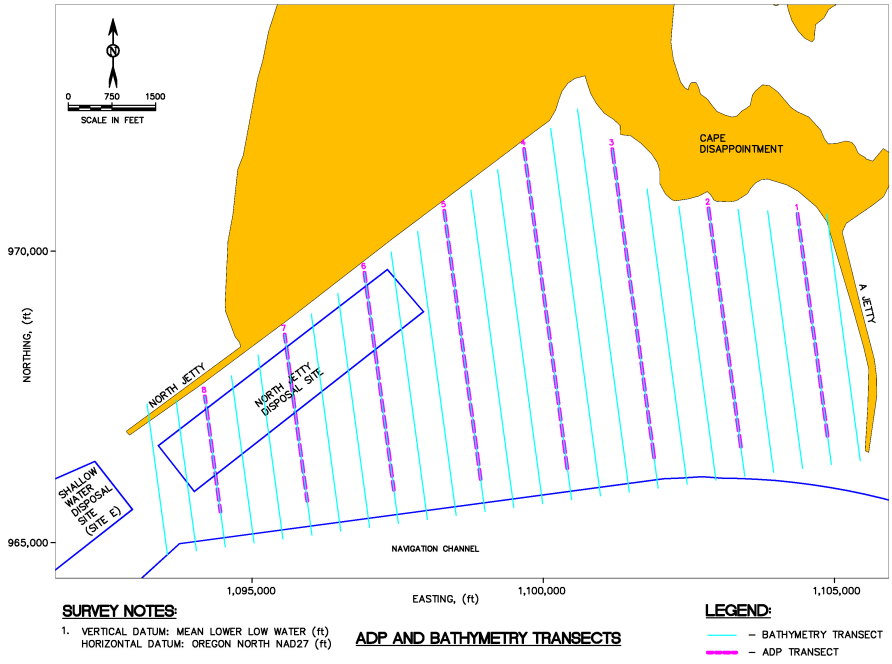

Figure 6 Roving ADP and bathymetry survey transects

ADP transects 8 transects with total length of approximately 15,000 ft (4500 m) and transect spacing of 1500 ft.

25 bathymetry transects were surveyed with spacing of 500 ft on 13 August 2003. The depth measurements were quality checked and incorporated with survey data collected by the US Army Corps of

Engineers to generate a high resolution digital elevation model (DEM). A 3-dimensional projection of the DEM is included in Appendix A.

4. Results

4.1. Waves

4.1.1. Wave Measurements at Columbia River Bar

Measurements of significant wave height (H_s), peak period (T_p), average period (T_{av}), and peak wave direction (*DIR*) from the directional wave gauge at the Columbia River Bar (NDBC 46029) were compiled and analyzed. The inter-relationship between H_s and T_p is relevant to a dredged sediment re-handling operation because the potential for unsafe operating conditions depends on the wave height and period at the site. The *DIR* of waves is a factor controlling wave height at the site because of the sheltering effects of the north jetty. The variations and trends in deep-water waves also influence the dynamics of the MCR entrance area by modifying current patterns and through the entrainment and transport of bottom sediment. A joint H_s - T_p distribution for all waves measured at the buoy between 5 September 1995 and 31 August 2003 (the time period for which direction measurements are available) is shown in Figure 6. The joint distribution shows that H_s up to 11 m and T_p up to 22 sec can occur in deep water at MCR. However, most of the time, H_s is less than 3 m with corresponding T_p between 8 and 12 sec. The longest period waves correlate with H_s of 2 to 3 m while the highest waves correlate with somewhat shorter periods. Similar joint distributions for the summer dredging season (July – September) are also shown in Figure 6.

Time series of monthly statistics of H_s, T_p, and *DIR* for the period 1984 to 1987 and 1991 to 2003 measured at NDBC 46029 are shown in Figure 7. There is a strong seasonal variation in the wave climate of the eastern north Pacific (e.g. Allan and Komar, 2002; Osborne, 2003) and this pattern is evident in the statistical plots shown in Figure 7 and in the joint H_s - T_p distributions in Figure 6. Monthly average H_s is a minimum (less than 1.5 m) during July and August compared with a winter maximum (more than 3 m) during November through January. Wave period exhibits a similar seasonal variation to wave height, averaging less than 10 sec in summer and increasing to more than 12 sec in winter. There is also a marked seasonal variation in *DIR*, with summer waves predominately from the northwest and west-northwest while winter storm waves mostly originate from the west-southwest and southwest.

Inter-annual variations in monthly H_s measured at NDBC 46029 for summer months over the past three years are shown in Figure 8. The inter-annual variations in H_s over the last several years have generally been within 10 percent of the long-term averages for those months. The maximum H_s measured at NDBC 46029 during the summer dredging season (July through September) for the period 1995 to 2003 is 6.6 m with corresponding T_p of 17.4 sec occurring on September 27, 1997. The average summer storm for this interval has a maximum H_s of 4.5 m with T_p of 12.7 sec, and *DIR* of 268 deg.

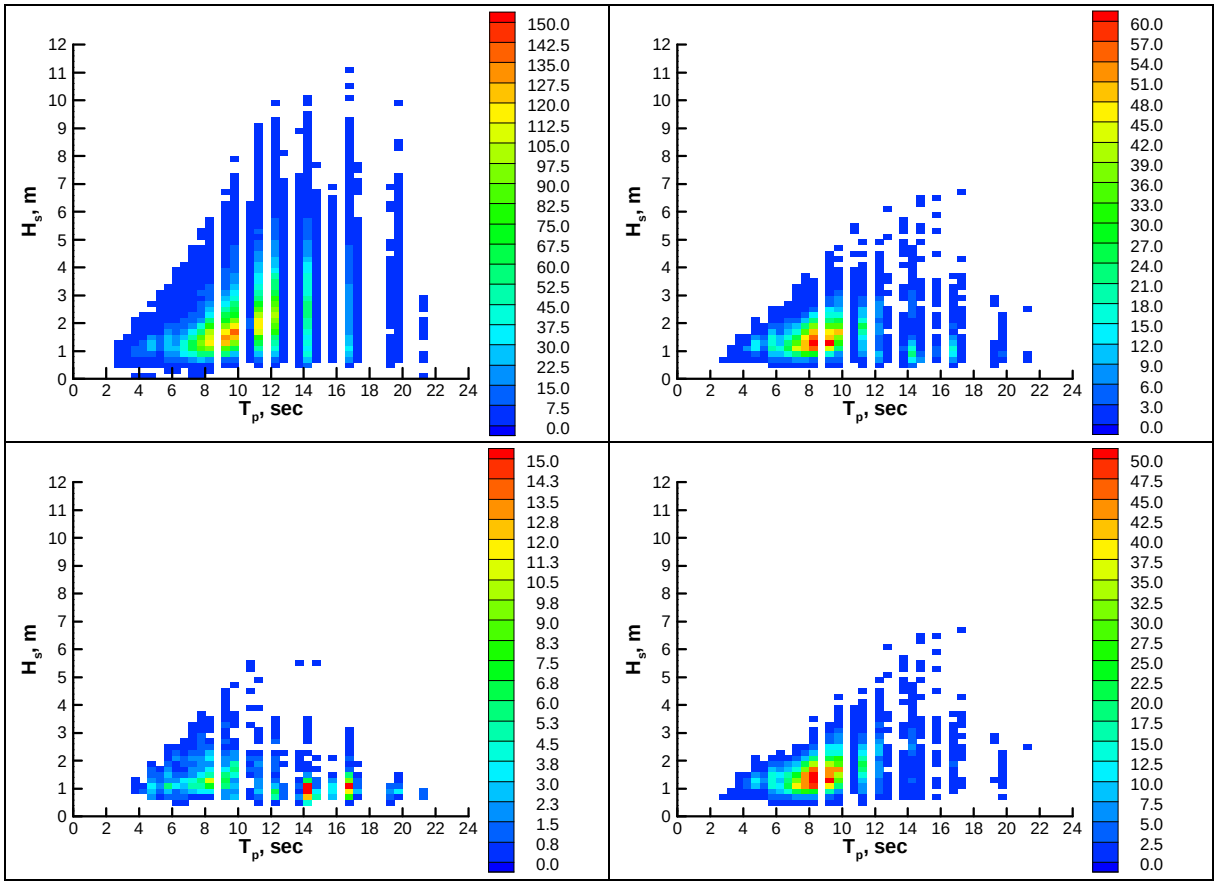

Figure 7 **Joint H_s - T_p distributions showing hours of occurrence for waves measured at NDBC 46029 between 1995 and 2003. Top Left: all waves from all directions; Top Right: Summer waves from all directions; Bottom Left: Summer waves from 180 to 270 deg; Bottom Right: Summer Waves from 270 to 360 deg.**

4.1.2. Waves at North Jetty

Waves reaching the project area to the south of north jetty from the Pacific Ocean are subject to shoaling, refraction, and diffraction by changes in bathymetry both outside and inside the MCR entrance, by interaction with tidal currents in the entrance, and by interaction with structures including the north jetty and jetty A.

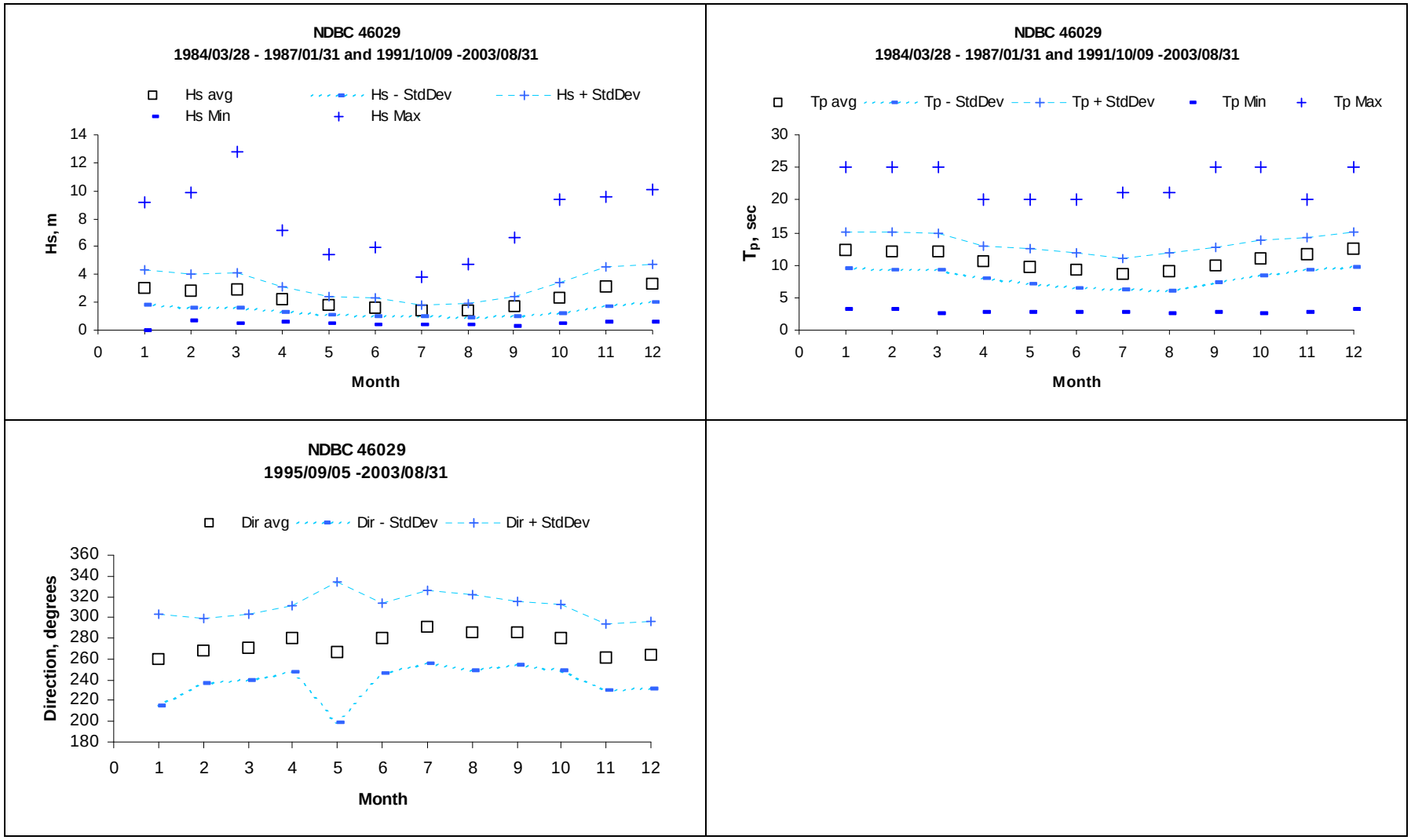

Figure 8 Monthly statistics of H_s , T_p , *DIR* measured at NDBC 46029 for the period 1984 to 1987 and 1991 to 2003

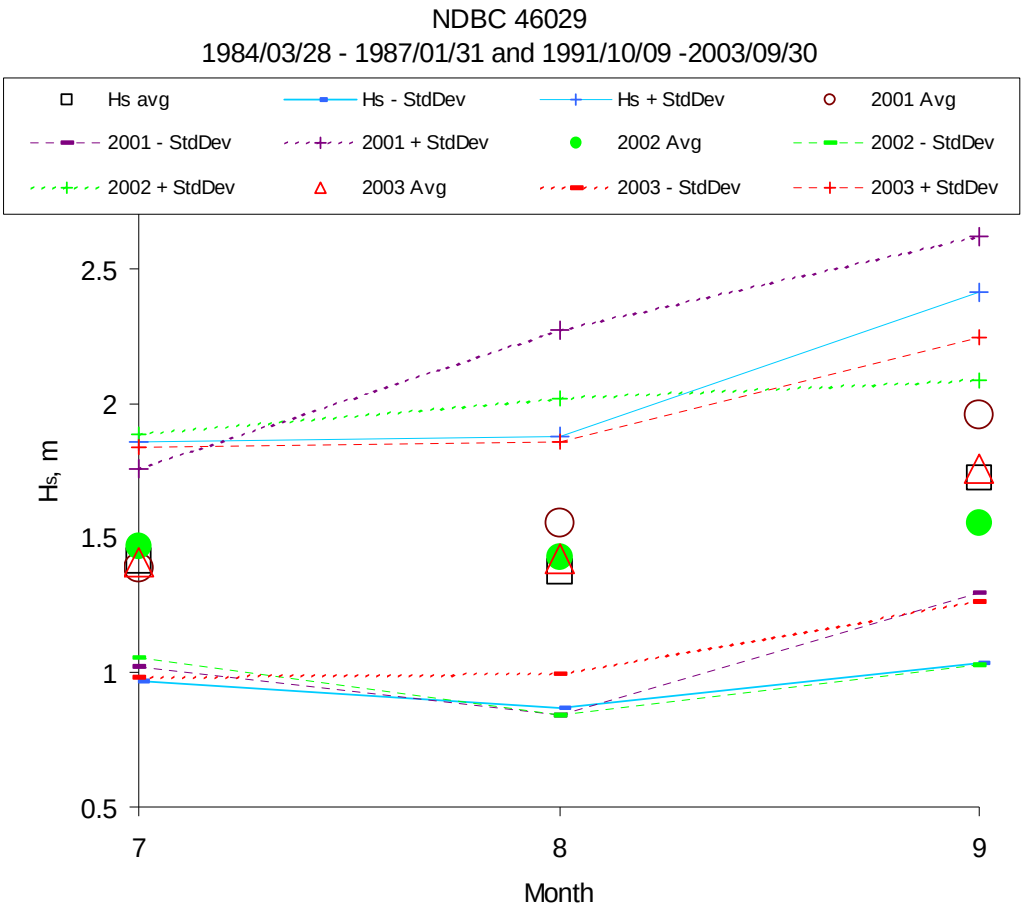

Figure 9 **Inter-annual variation in monthly H_s statistics for July through September measured at NDBC 46029**

A time series of wave spectra (water surface variance density as a function of frequency) measured at Station 2 (RDI-ADCP) between July 25 and September 18, 2003 is shown in Figure 10. The spectra reveal a gradual increase in spectral energy over time between July and September with peak energy occurring in the 8-12 sec range. There is a diurnal and semi-diurnal modulation of the spectral energy in the time series that correlates with tidal variations in both local water depth and current as well as a longer term variation associated with wind forcing (and wave height). The spectra become broader and more intense during wind forced wave conditions. The tidal variations in waves are further illustrated in Figure 11 which shows a short time series of H_s and depth measured at Station 2. H_s increases during the falling tide (ebb currents and decreasing water depth) reaching a maximum just prior to low tide and decreases on a rising tide (flood currents

and increasing depth) reaching a minimum at approximately high tide.

Locally, wave spectra are also influenced by wave-structure interactions that include refraction, diffraction, and reflection. A typical directional spectrum measured by the RDI-ADCP at Station 2 is shown in Figure 12. In this case, incident variance is broadly distributed between approximately 180 and 270 deg with a well-defined peak in wave direction occurring at approximately 247 deg. Variance is also broadly spread in frequency space with T_p occurring at 10.6 sec. A smaller but significant peak in wave energy is also evident at the same peak frequency as the incident waves but approaching from approximately 50 deg. This secondary peak is interpreted as reflected wave energy from jetty A to the east of Station 2. The *DIR* measured concurrently at NDBC 46029 with the spectrum shown in Figure 12 was 274 deg, indicating that the incident waves have turned approximately 30 deg to a southwesterly approach by the time they arrive inside the entrance to MCR at Station 2. This rotation is caused by diffraction of the waves on the tip of north jetty and by refraction of the waves as they propagate along the jetty and across the entrance bathymetry.

Time series of wave parameters measured at Station 2 during the entire summer 2003 deployment are shown in Figure 13. The time series shown in Figure 13 compare wave parameters determined with the SonTek Hydra directional wave gauge and the RD Instruments directional wave gauge. The time series indicate a reasonable level of agreement between the different sources of wave data. The RDI estimates of H_s are 11.3 percent higher on average than the corresponding Hydra estimates; this discrepancy is most likely mainly attributable to errors in the correction of attenuation of the pressure velocity measurements. The RDI wave gauge uses four independent estimates of surface elevation; the results are therefore considered to be more robust than the bottom mounted *p,u,v* estimates from the Hydra. The RDI estimates of T_{av} are approximately 16.8 percent lower than the Hydra estimates while the RDI estimates of *DIR* are 17.5 percent higher than the Hydra estimates.

Time series of H_s and *DIR* measured at Stations 1, 2, and 3 near north jetty and at NDBC 46029 between July 25 and September 18, 2003 are shown in Figure 14. There is a qualitative correlation between the measurements at all four locations with the largest waves occurring in deep water at the NDBC buoy and progressively smaller waves occurring at Stations 3, 2 and 1 in the MCR entrance. Larger waves occur at Station 3 relative to Station 2 because Station 3 is located slightly further south, away from the

protection of the north jetty, and therefore more exposed to the Pacific Ocean swell. Time series of *DIR* are less well correlated between NDBC 46029 and Stations 2 and 3 although there is generally good agreement between Stations 2 and 3. *DIR* measured at NDBC 46029 is generally larger (more northerly approach) than at Stations 2 and 3 except when waves approach from angles south of 260 deg, in which case the *DIR* in the entrance is closer to the offshore *DIR*. This suggests that the waves approaching from north of 260 deg are modified significantly by refraction and diffraction at the north jetty and by bottom topography in the entrance. The time series confirm that in summer, waves are predominately from north of west, and therefore the north jetty shelters the area immediately south of the jetty resulting in both a change in wave direction and a significant reduction in wave height.

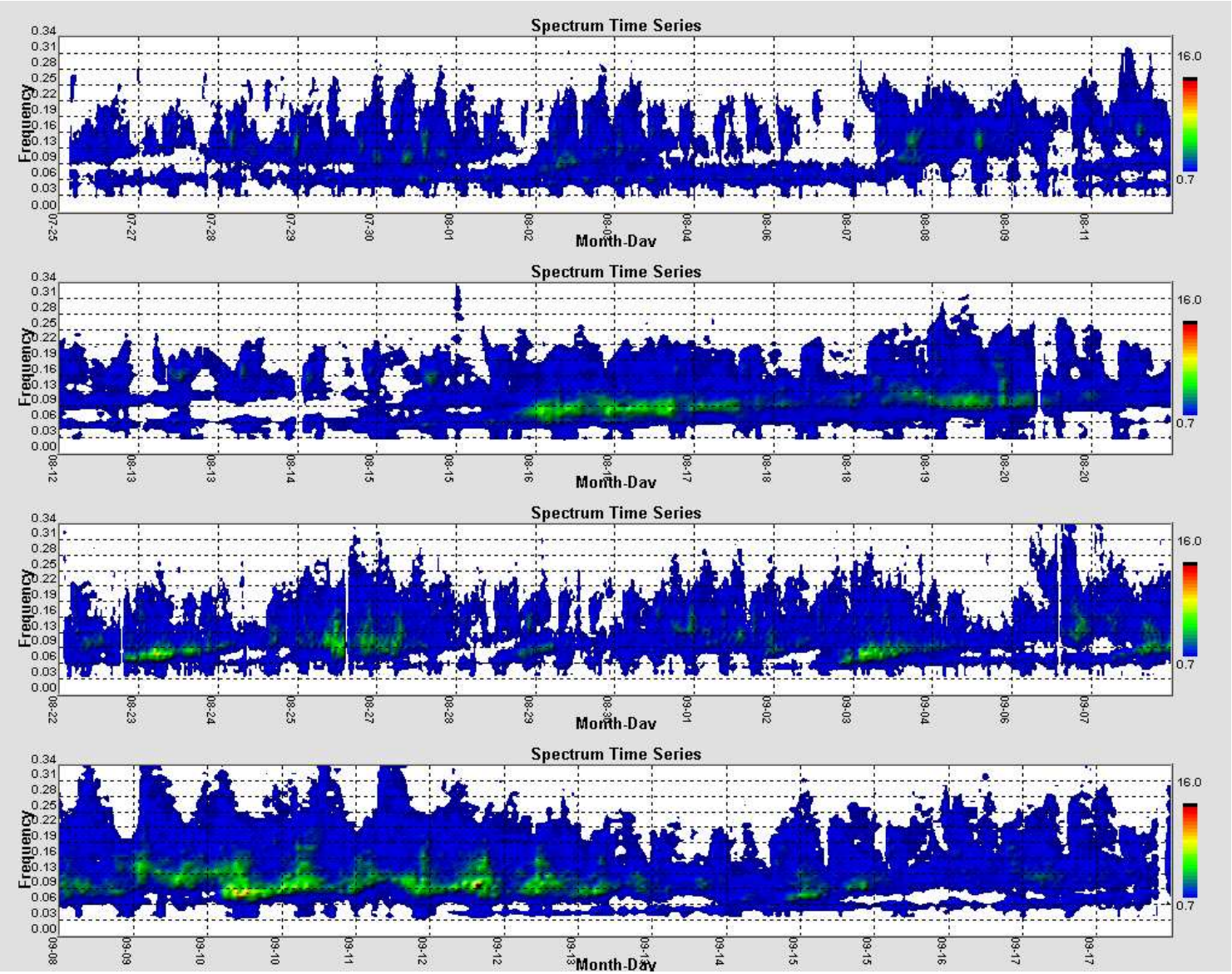

Figure 10 Wave spectrum time series for Station 2 from July 25 through September 18, 2003

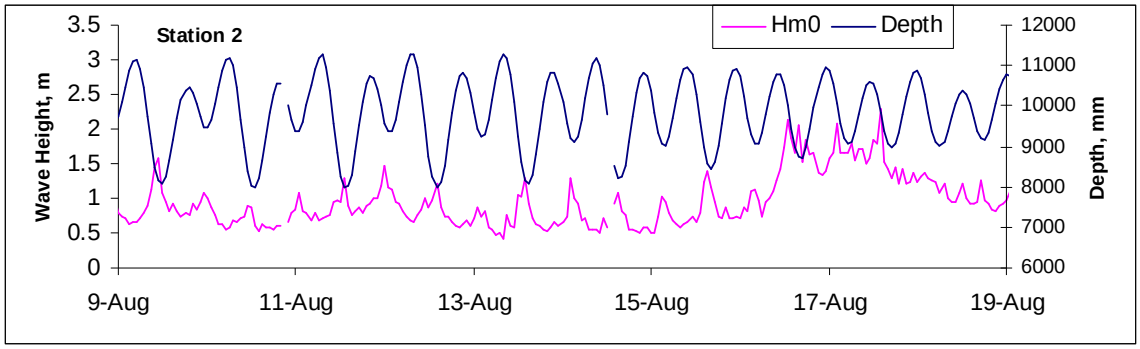

Figure 11 **Time series of Hs and depth measured at Station 2 between August 9 and August 19, 2003**

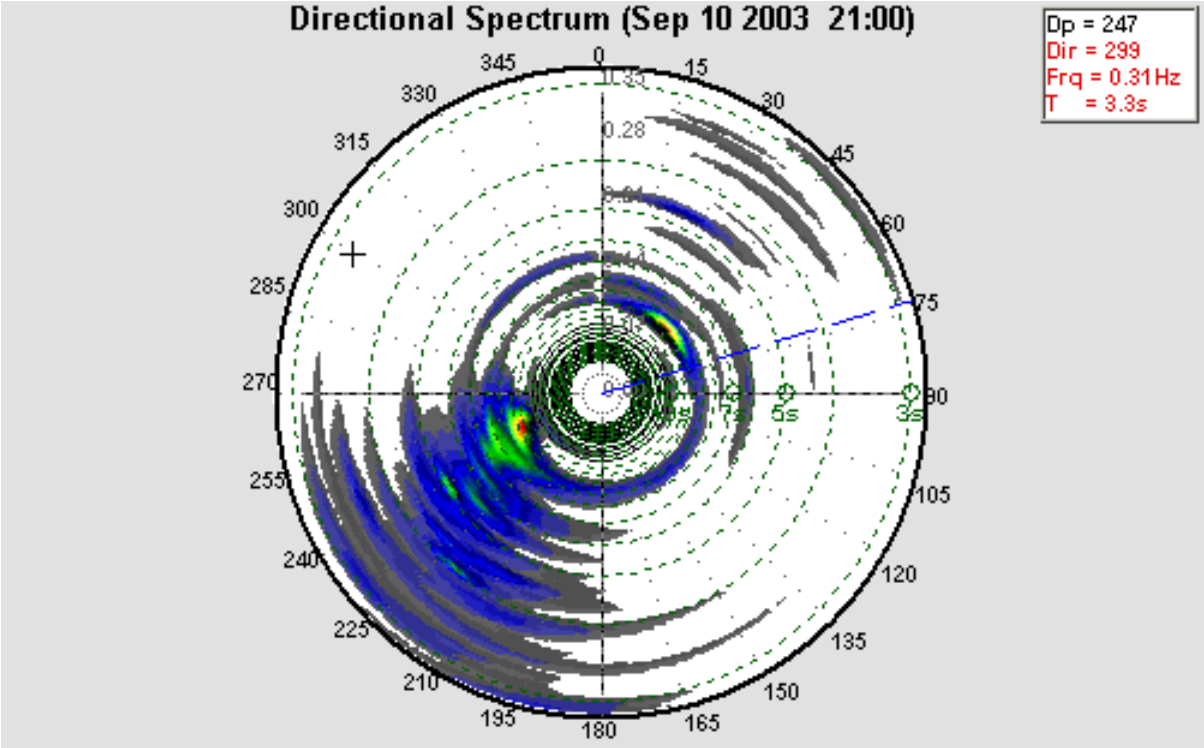

Figure 12 **Directional spectrum measured at Station 2 for September 10, 2003 at 21:00 UTC**

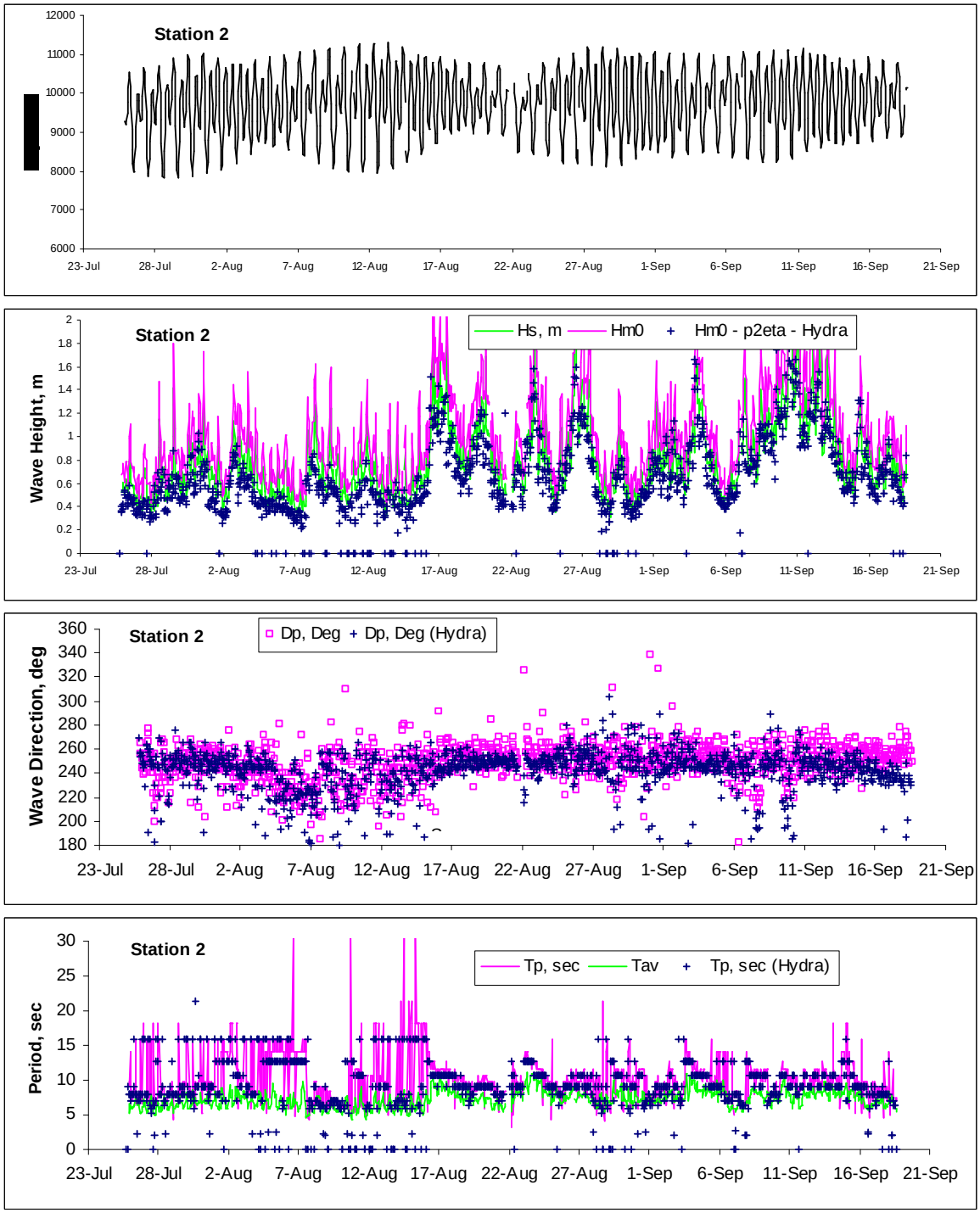

Figure 13 **Time series of water depth, wave height, wave direction and wave period measured at Station 2 by the RDI ADCP and the SonTek Hydra systems**

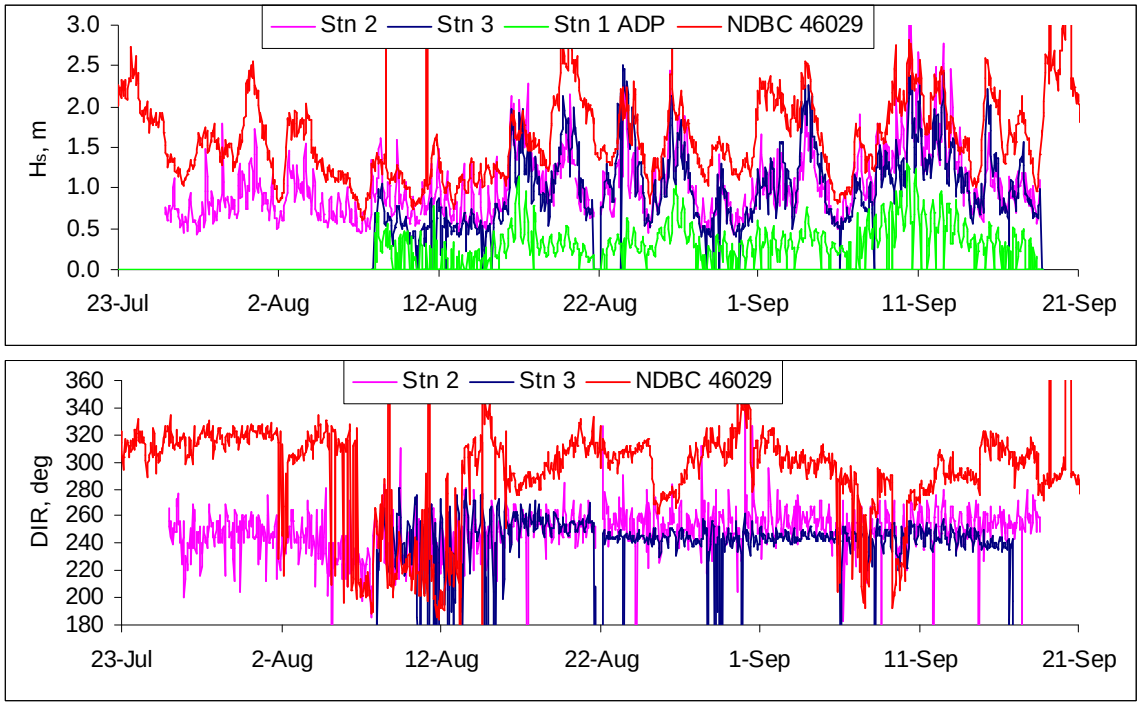

Figure 14 **Time series of *H_s* and *DIR* measured at Stations 1, 2, and 3 near north jetty and at NDBC 46029 between July 25 and September 18, 2003**

Figure 15 shows wave height distributions measured at Station 1 and NDBC 46029 between July and September for 2000, 2002, and 2003. The wave height distributions indicate that H_s is less than 0.5 m (1.6 ft) at Station 1 more than 50 percent of the time whereas H_s is greater than 1 m (3.3 ft) more than 90 percent of the time in deep water at NDBC 46029. Wave height distributions at Station 1 are similar for three years of measurement (2000, 2002, and 2003).

Figure 16 shows wave height exceedance curves for the three stations south of north jetty and NDBC 46029 for summer month measurements in 2003. Summer month measurements for Station 1 are also shown for 2000 and 2002. H_s has exceeded 1 m (3.3 ft less than 5 percent of the time at Station 1 during each of 2000, 2002, and 2003 summer dredging seasons. H_s exceeds 1 m (3.3 ft) less than 50 percent of the time at Stations 2 and 3, and almost 90 percent of the time at NDBC 46029 during the 2003 summer dredging season.

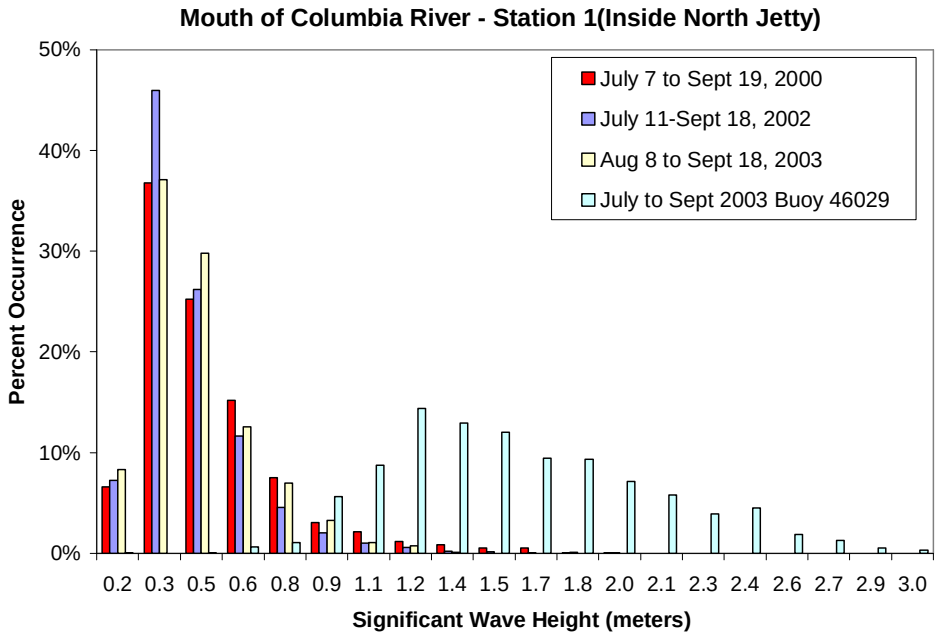

Figure 15 **Wave height distributions between July and September at Station 1 (2000, 2002, and 2003) compared with NDBC 46029 for the same period**

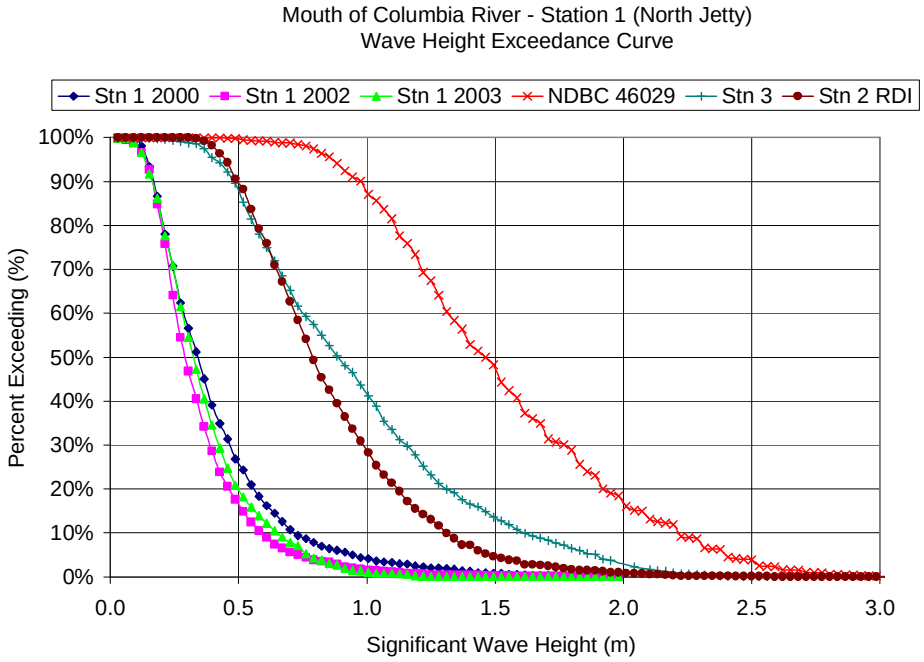

Figure 16 **Wave height exceedance curves for Station 1, 2, and 3 and NDBC 46029 for July through September**

4.2. Currents

4.2.1. Near Bottom Currents and Suspended Sediment at North Jetty

Currents at MCR north jetty are forced by a number of mechanisms including tidal processes, Columbia River discharge, salinity variations, and local, regional, and global scale meteorological processes. The semi-diurnal tidal currents dominate the current regime in this part of the estuary except possibly during periods of high river discharge. Wind and wave driven currents also influence the flows in the area near north jetty. Current measurements were collected to examine the potential constraints on a dredged sediment re-handling operation at north jetty and also to examine the potential sediment transport regime under existing conditions. Current measurements were collected as near bottom measurements and velocity profiles throughout the water column at each of the three measurement stations and also by ADP mounted on a moving vessel during two successive tidal cycles.

Figure 17 shows current roses for time-averaged near bottom currents measured by the ADVO at Stations 1, 2, and 3 overlaid on a base map of the MCR. The averaging interval of each data point is approximately 34 minutes (1 burst). The current roses indicate that the dominant (most frequent and highest) speeds are to the east-northeast at Station 1 and Station 2, and to the east-southeast at Station 3. Time-averaged near bed current speeds rarely exceed 0.5 m/sec at these locations.

Figure 18 shows a short time series of hourly burst-averaged water depth and near-bottom current speed measured at Station 2. The measurements indicate that maximum current speeds occur during a rising tide and therefore the tidal current is flood-dominated at this location. The maximum ebb-phase currents in this area, south of north jetty, are generally about half the speed of the maximum flood currents. A short duration slack occurs just after each high tide and each low tide. The distinctive diurnal inequality in tidal elevation is evident in the time series of water depth and velocity.

Figure 19 shows vector plots of near bottom velocity with plots of water depth, and H_s, for one week during the deployment. The orientation of each vector from the origin on the x-axis shows the direction of current flow and the length of the vector is scaled proportional to the current speed. The vector plot indicates that the bottom current flows in a counterclockwise elliptical path in each tidal cycle at this location with the strongest flows occurring during the flood tide. Current vectors are also modulated by variations in H_s.

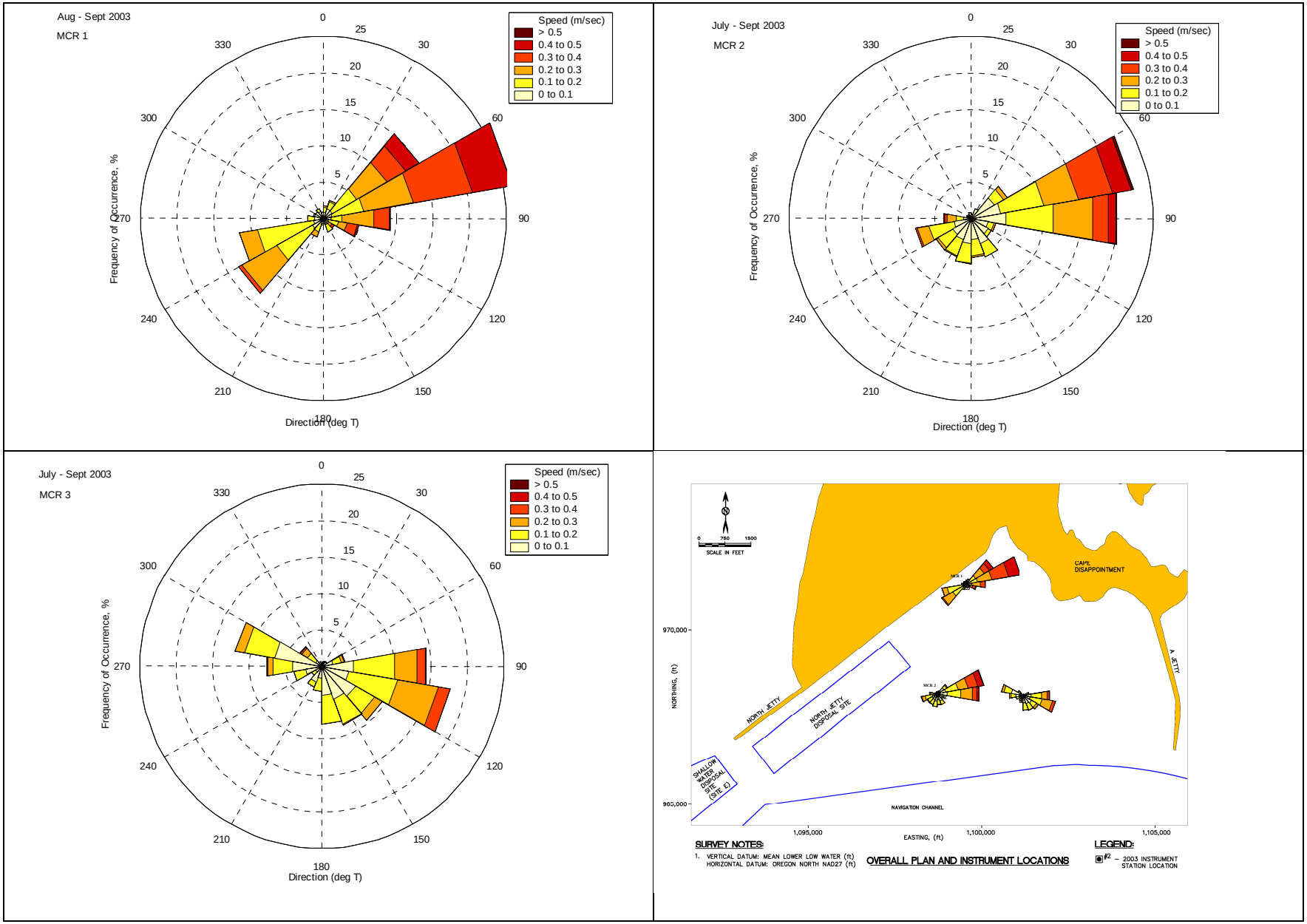

Figure 17 Near bottom current roses for Station 1 (top left), Station 2 (top right), and Station 3 (bottom left)

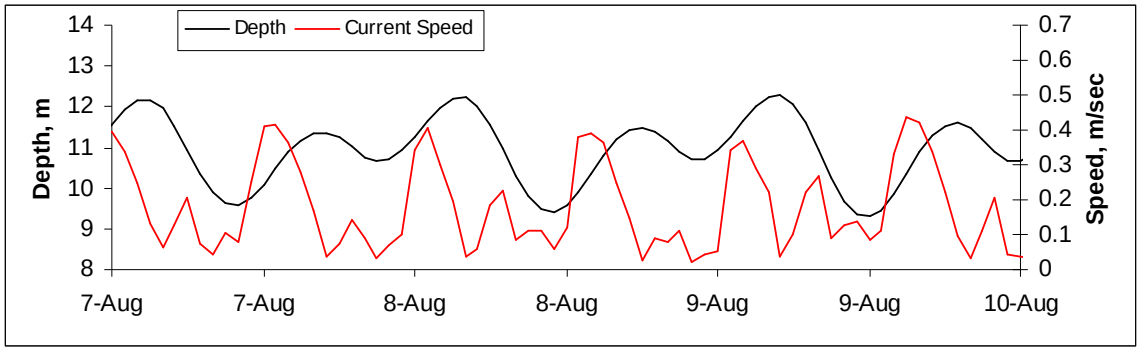

Figure 18 **Time series of water depth and current speed at Station 2 over a 3-day period**

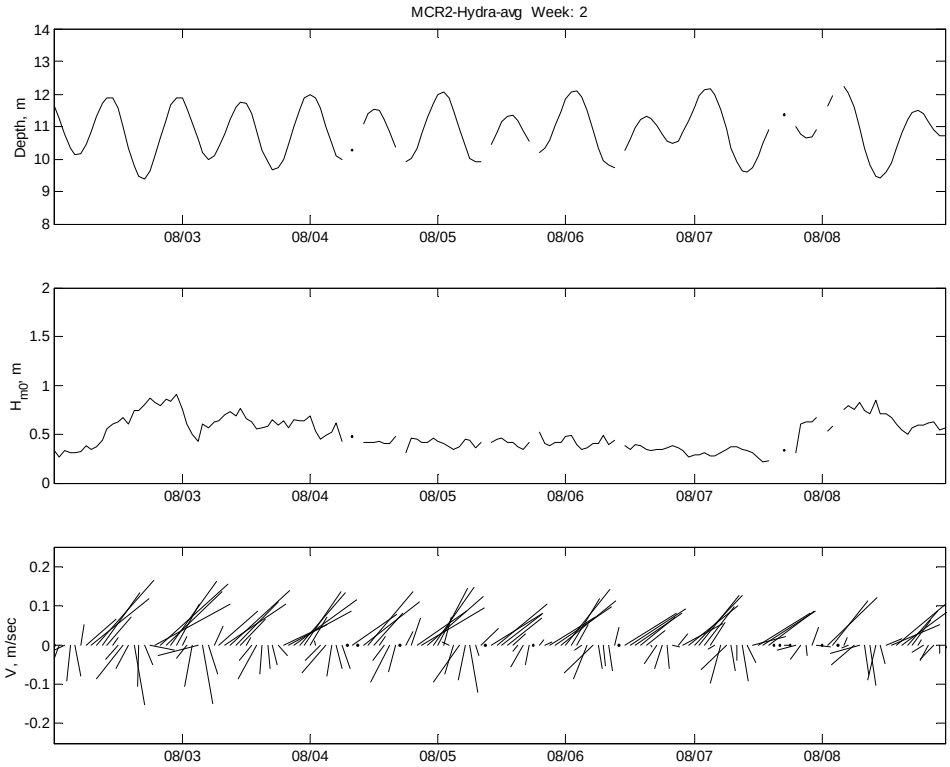

Figure 19 **Time series of water depth, H_s, *V*, *SSC*, and velocity measurement elevation at Station 2**

Figures 20 and 21 show time series of current speed, wave orbital velocity, bed shear stress, *SSC*, and height of the velocity measurement relative to boundary through the deployments at Stations 2 and 3. The variations in SSC correlate approximately with the variations in the maximum bed shear stress due to combined waves and currents. SSC is correlated with both tidal phase and with H_s at this location. An increase in SSC, particularly at the bottom OBS sensor is evident during, and for a few days following, periods of high wave orbital velocities. This

indicates enhanced re-suspension, particularly of fine sediments with low fall velocity, during periods of wave action. Small peaks is SSC also correspond with peak ebb flow as low water is approached, although the apparent tidal modulation may be related to the tidal modulation in wave height as discussed above rather than the variation in mean current speed with tidal phase.

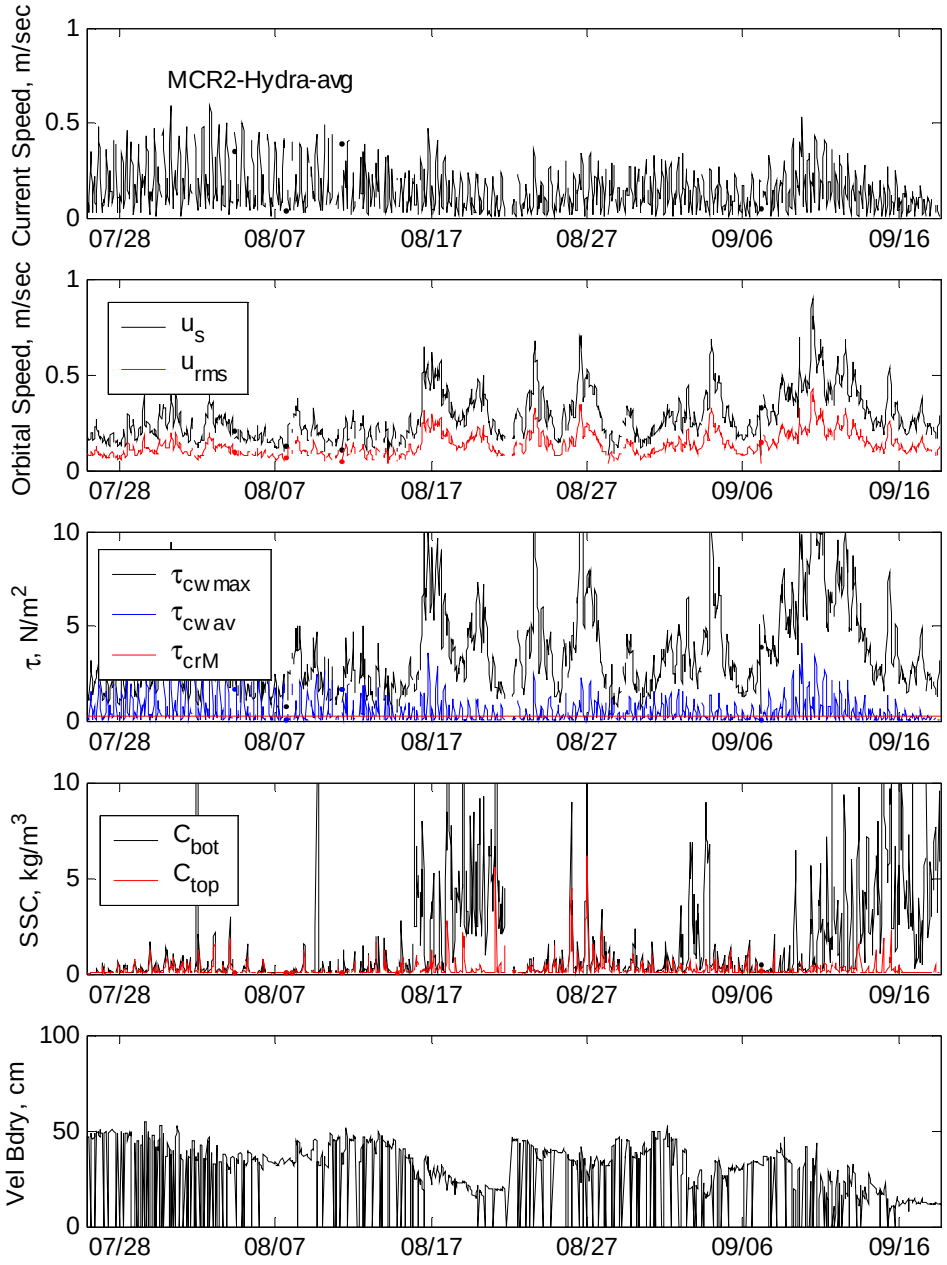

Figure 20 Time series of current speed, wave orbital elocity, bed shear stress, SSC, and height of

velocity measurement relative to boundary at Station 2

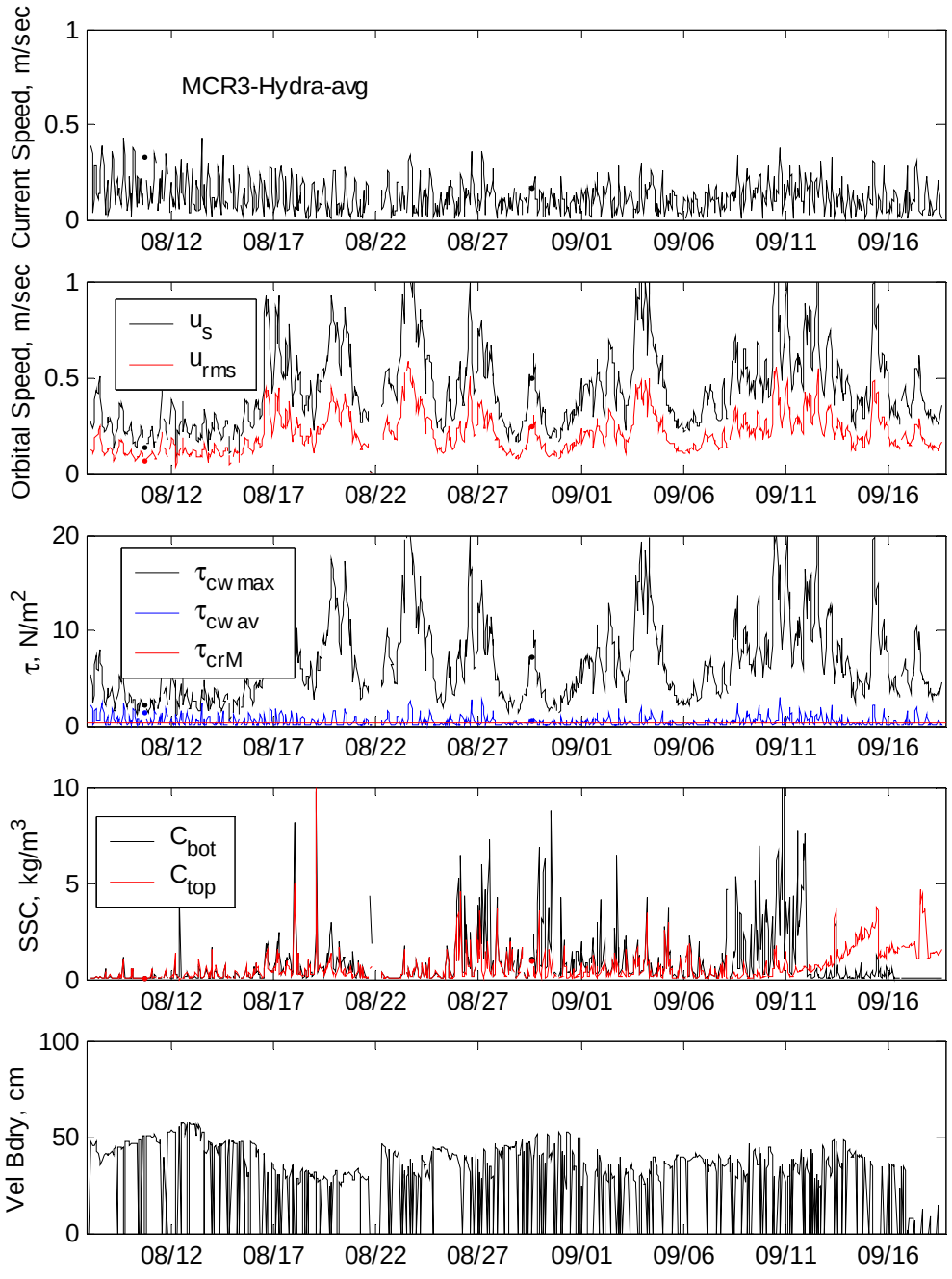

Figure 21 **Time series of current speed, wave orbital velocity, bed shear stress, SSC, and height of velocity measurement relative to boundary at Station 3**

4.2.2. Three-dimensional and Depth-averaged Circulation at North Jetty

The tidal range at MCR is 2.6 m (8.5 ft) and instantaneous flow can exceed 40,000 cms (1.5 mcfs) during the ebb tide (Moritz et al. 2003). Between the north and south jetties the strength of tidal forcing increases relative to storm- and wave-driven currents. Peak ebb and flood currents inside the entrance vary mainly with tidal range and river discharge. At the entrance, currents are also constrained by bathymetry and the presence of three jetties.

Three-dimensional views of synchronous current vector transects in the area between jetty A, north jetty, and the navigation channel during various phases of a spring tidal cycle (12-13 August 2003) are shown in Figures 22 through 29. Corresponding maps of depth-averaged current vectors are shown in Figures 30 through 37. Peak ebb and peak flood currents reach 2.3 m/sec (depth-averaged speeds of 1.0 m/sec) and flow essentially parallel with the navigation channel (Figures 23, 28, 31, and 36). The ebb current continues to flow at speeds up to 1.0 m/sec parallel to north jetty for up to an hour following low tide (Figure 22). A recirculation gyre with counter flows of up to 0.5 m.sec occurs in the northeast corner of the measurement area between Jetty A, Cape Disappointment, and the north jetty from peak ebb through low water (Figures 22, 28, 29, 30, 36, and 37). As the flood develops, the general flow is eastward and southeast between north jetty and cape disappointment. Jetty A constrains the flood causing it to turn southward and accelerate around the tip of jetty A where depth-averaged flows exceed 1.0 m/sec in more than 30 m of water (Figures 23, 24, 31, and 32). Later in the flood, currents in the northeast corner near Cape Disappointment slacken and a weak westward counter-flow develops (Figures 24, 25, 32, and 33). During late flood and early ebb, flows within 450 m north of the navigation channel continue to flow eastward into the entrance while the westward counter-flow along the jetties and near the Cape accelerates (Figures 25, 26, 27, 33, 34, and 35). A distinctive counterclockwise gyre is evident east of the tip of the north jetty during the late flood-to-high tide transition (Figures 25 and 33). At high slack a weak counterclockwise flow exists in the entire project area (Figures 26 and 34). As the ebb develops, the westward counter-flow diminishes and is replaced by an eastward recirculation in the northeast corner between North Jetty and Cape Disappointment (Figures 27, 28, 35, and 36). Depth-average flows on ebb and flood typically accelerate with distance from the jetty reaching peak flow speeds at distances more than 450 m from the structures.

Figures 22 through 37 illustrate that the major features of the north jetty circulation are reasonably well described by the depth-averaged vectors. Figures 38 through 41 depict the vertical and horizontal variations in the speed and direction of the current along several transects during various stages of the tide. A complete set of ADP transect cross-sections is included in Appendix B. During peak flood (Figure 38), the maximum flow speed is located several meters below the surface, possibly indicating the presence of a surface current influenced by wind or the presence of a lower density fresh water layer flowing in opposition to the saline flood current. In contrast the peak ebb current (Figure 40) is non-stratified in the vertical dimension and also uniform horizontally in terms of direction of flow. A relatively complex vertical structure in the flow can also occur, particularly during the late ebb and late flood stages. Figure 39 shows a view looking east of current speed and direction profiles along ADP transect 25 (located between the north jetty and navigation channel on the west end of North Jetty Disposal Site) during the transition from late flood to high tide. The cross-section indicates a core of higher velocity flow near the bottom starting approximately 600 m from the jetty on the edge of the channel. The faster, eastward-flowing bottom water represents higher density saline flow while the surface flow is slowed by the presence of freshwater with a tendency to flow seaward. In the late ebb (Figure 33), there is a weak eastward near bottom flow within 100 m of the jetty while flow at the surface is strongly westward at distances greater than 450 m from the jetty.

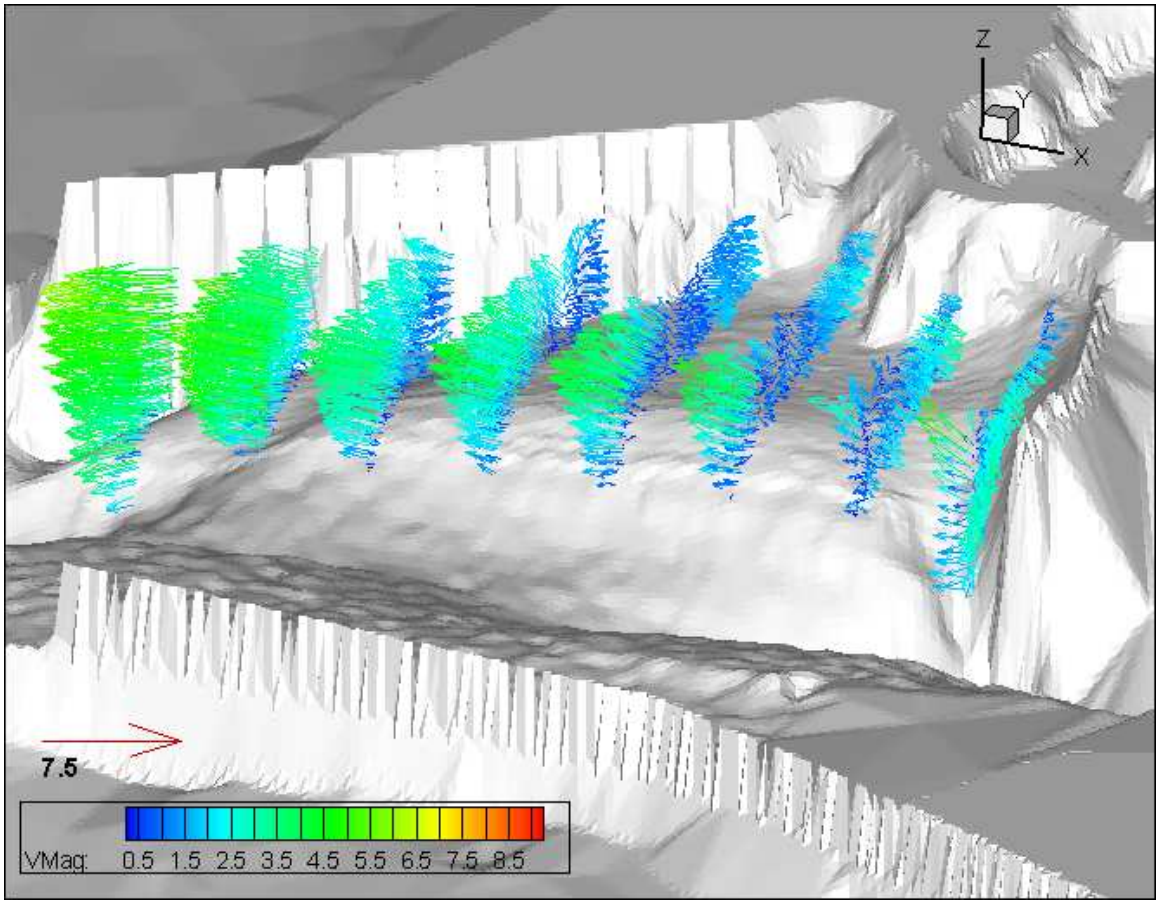

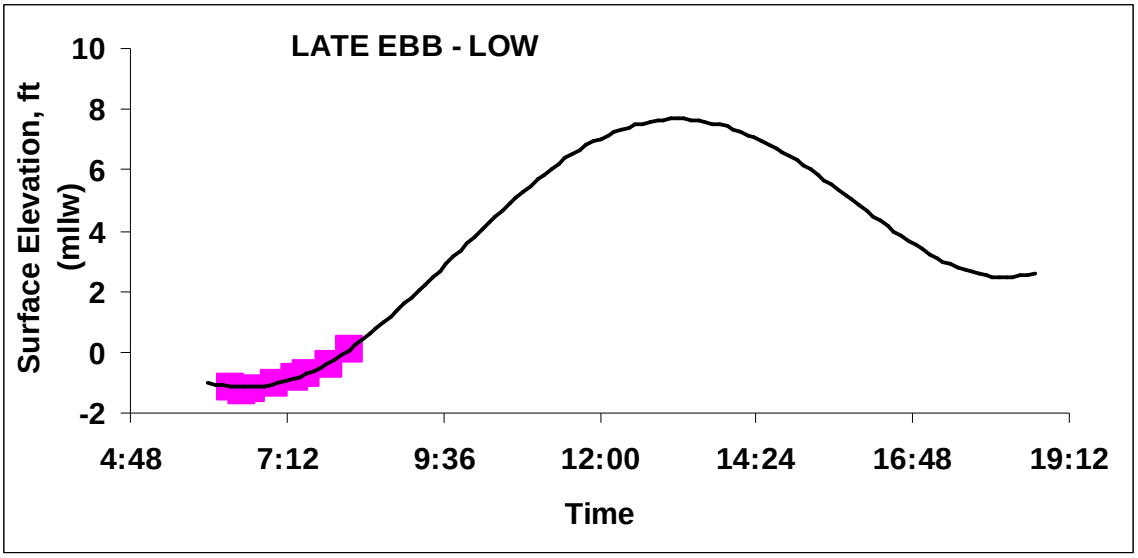

Figure 22 **Three-dimensional projection of the north jetty area with synchronous transects of three-dimensional velocity vectors at low tide on 13 August 2003**

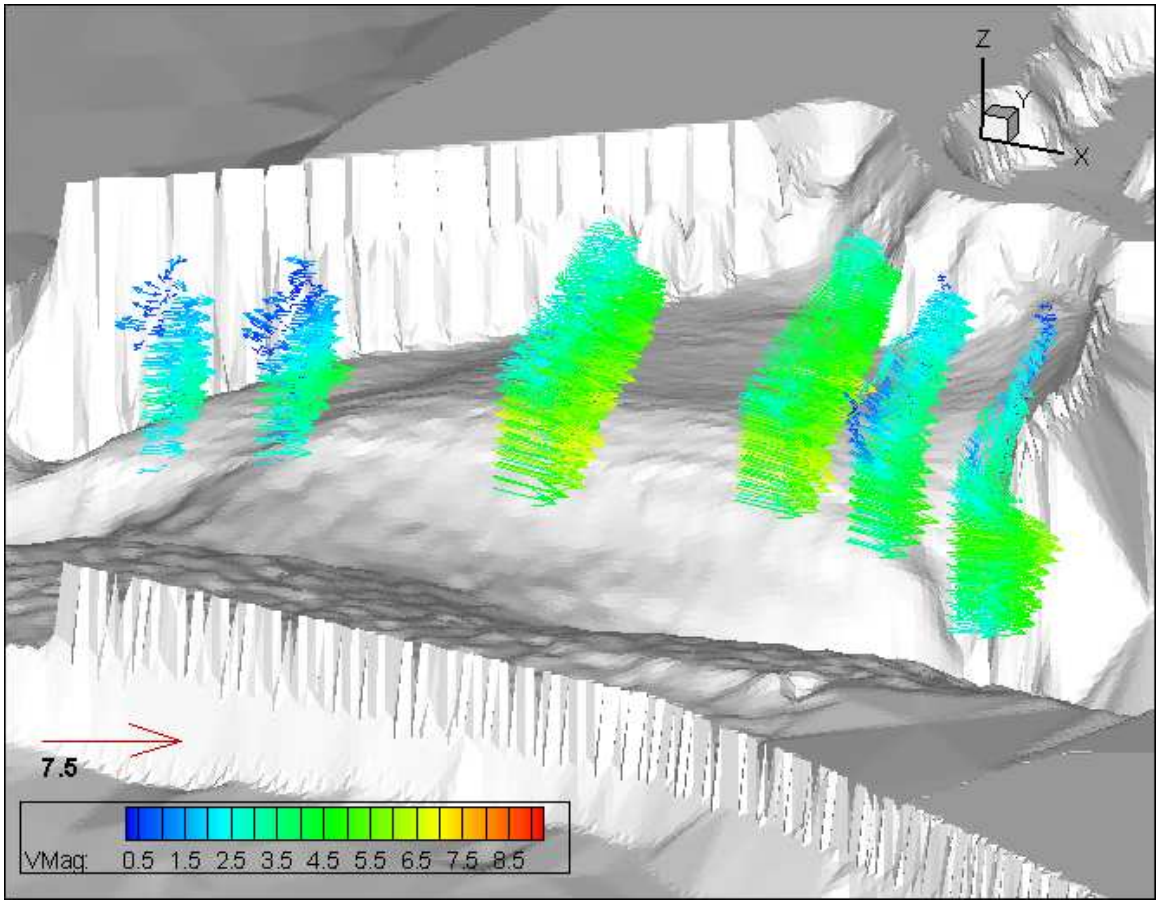

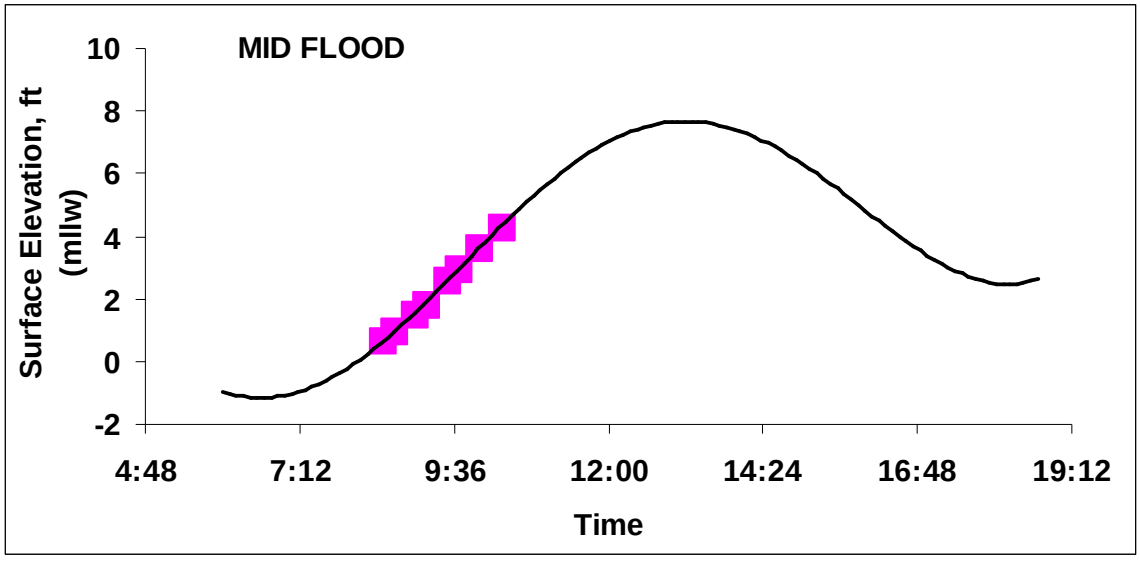

Figure 23 **Three-dimensional projection of the north jetty area with synchronous transects of three-dimensional velocity vectors during mid flood on 13 August 2003**

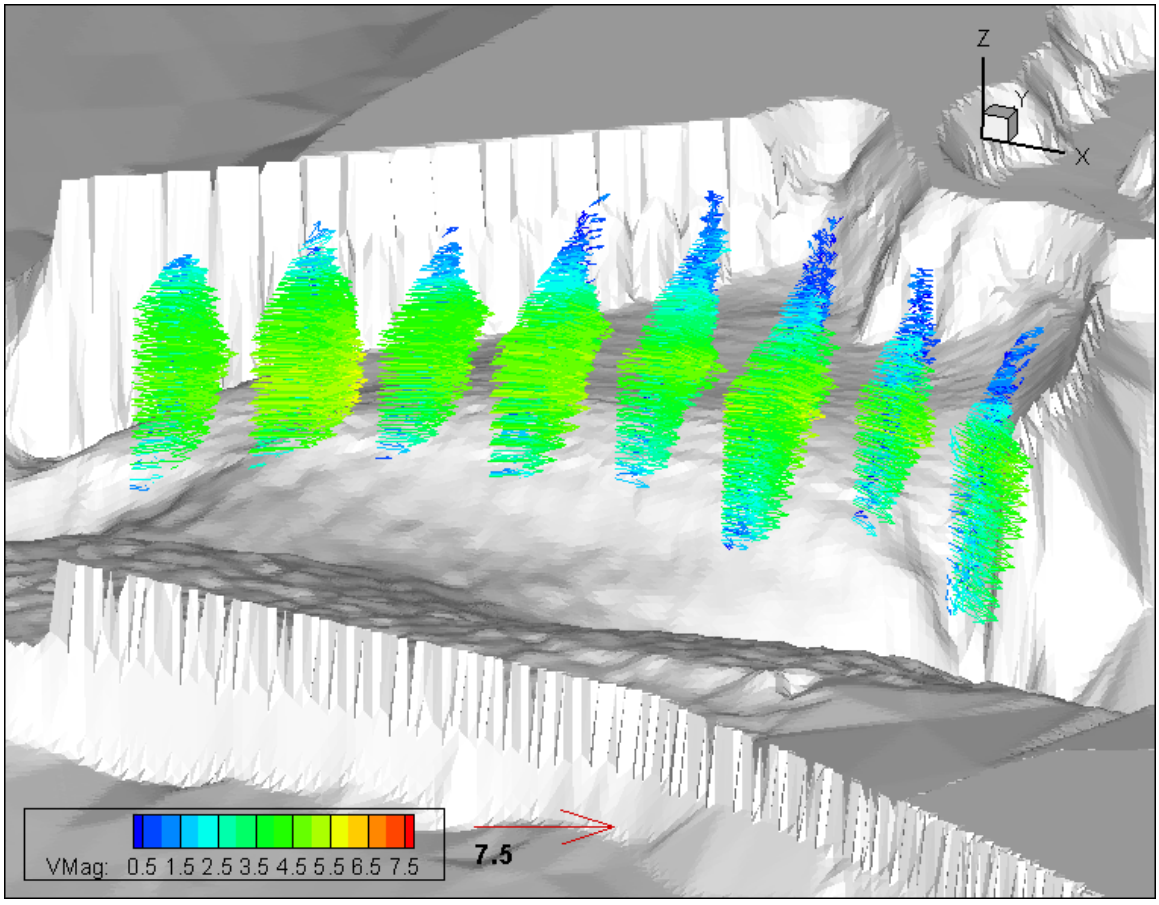

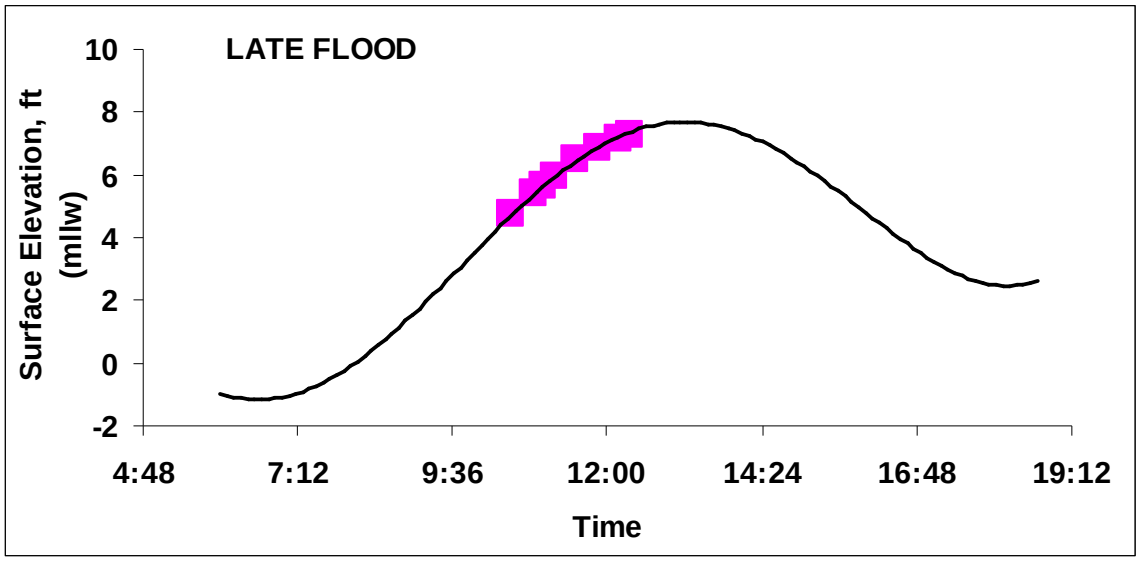

Figure 24 **Three-dimensional projection of the north jetty area with synchronous transects of three-dimensional velocity vectors during late flood on 13 August 2003**

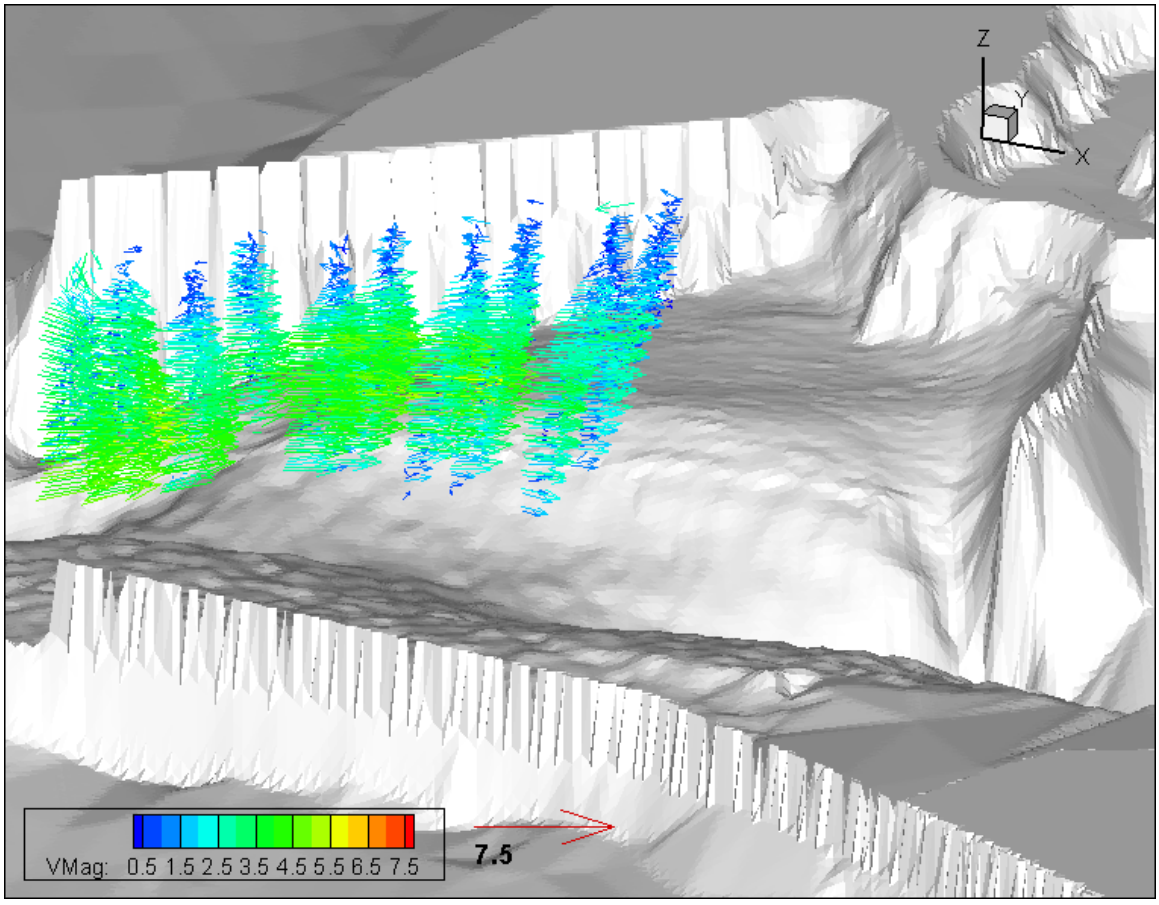

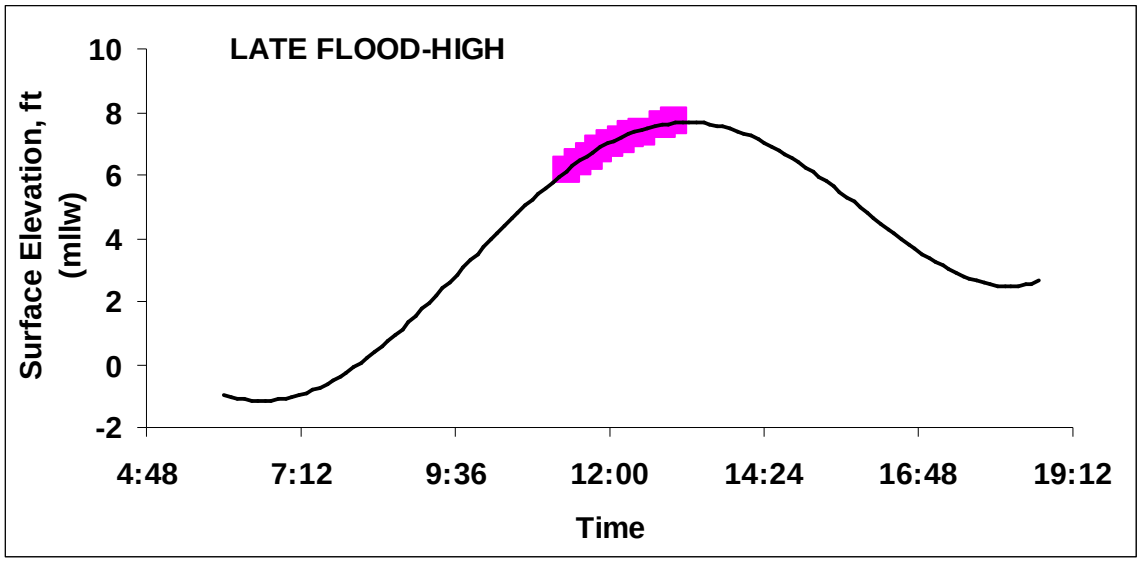

Figure 24 **Three-dimensional projection of the north jetty area with synchronous transects of three-dimensional velocity vectors during late flood to high tide on 13 August 2003**

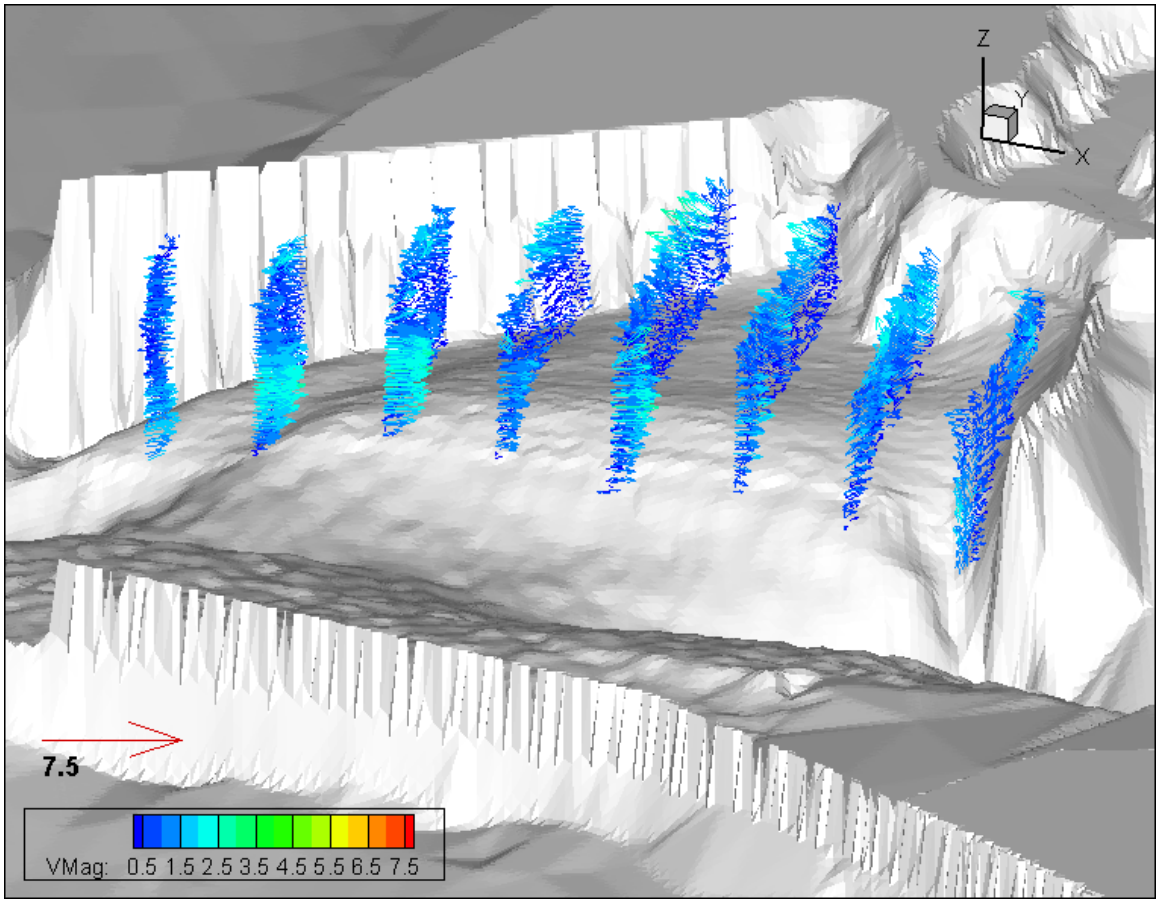

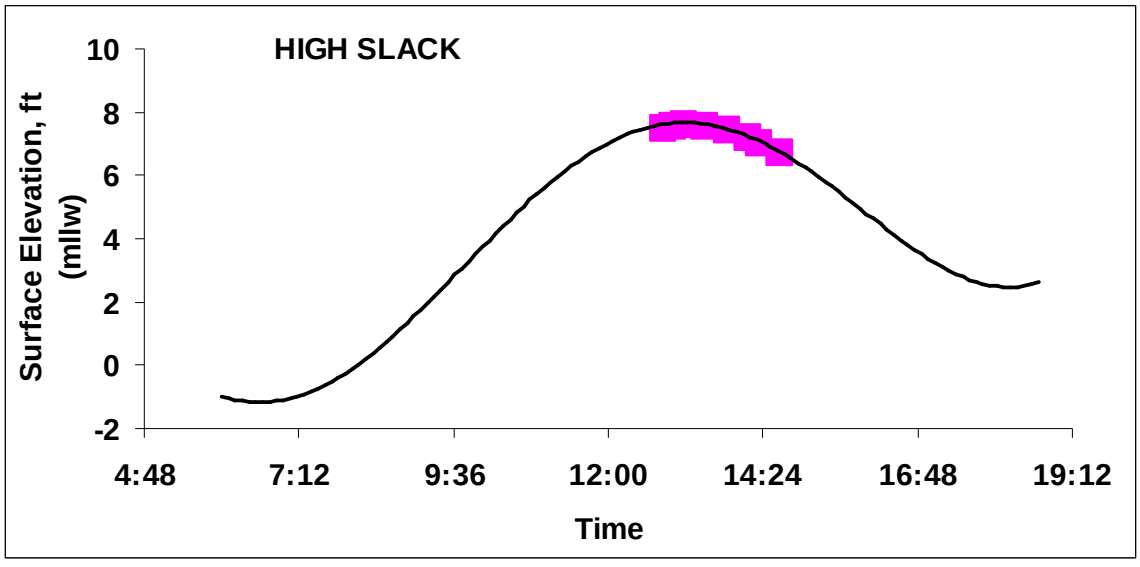

Figure 26 **Three-dimensional projection of the north jetty area with synchronous transects of three-dimensional velocity vectors during high tide slack on 12 August 2003**

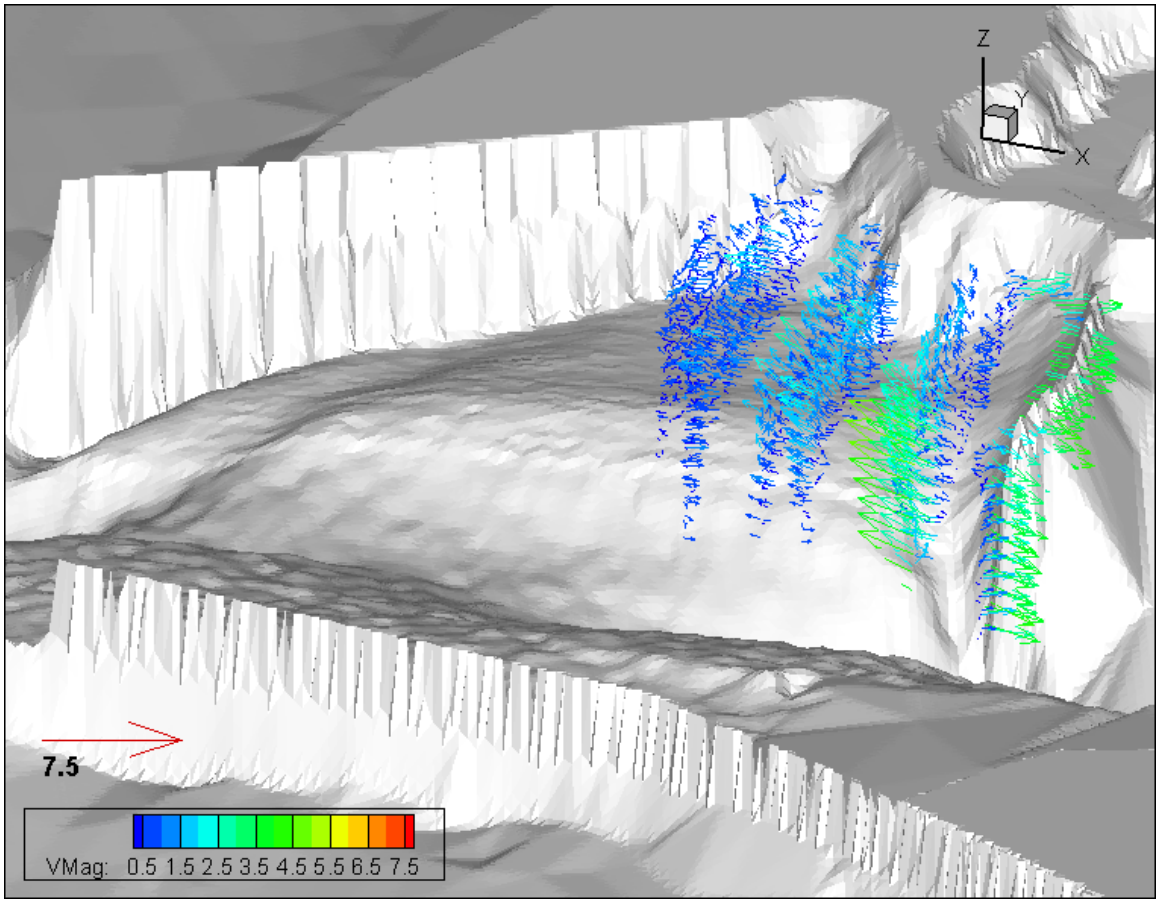

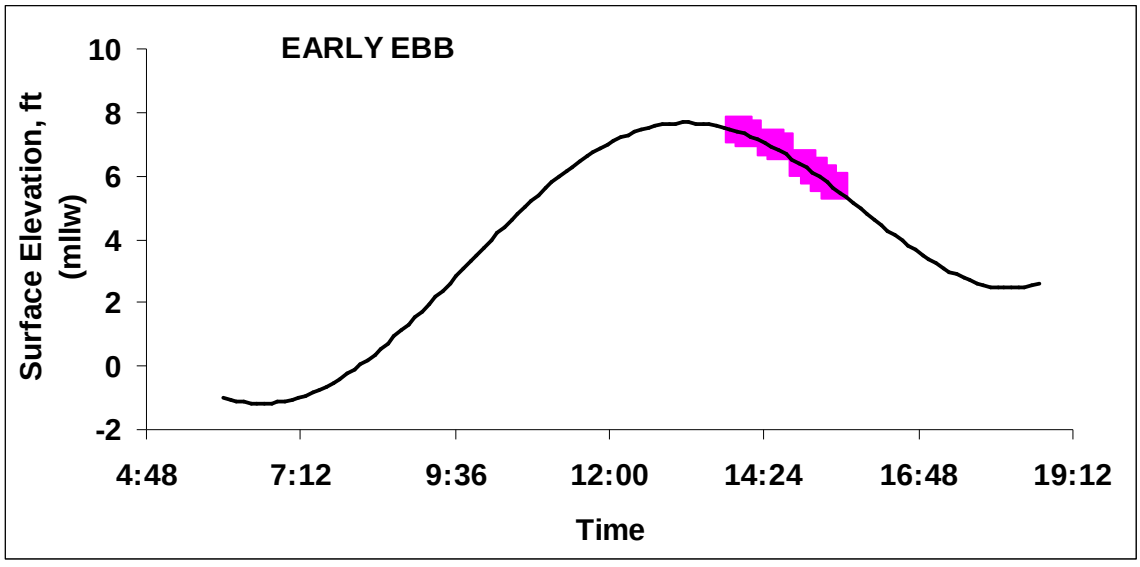

Figure 27 **Three-dimensional projection of the north jetty area with synchronous transects of three-dimensional velocity vectors during early ebb on 13 August 2003**

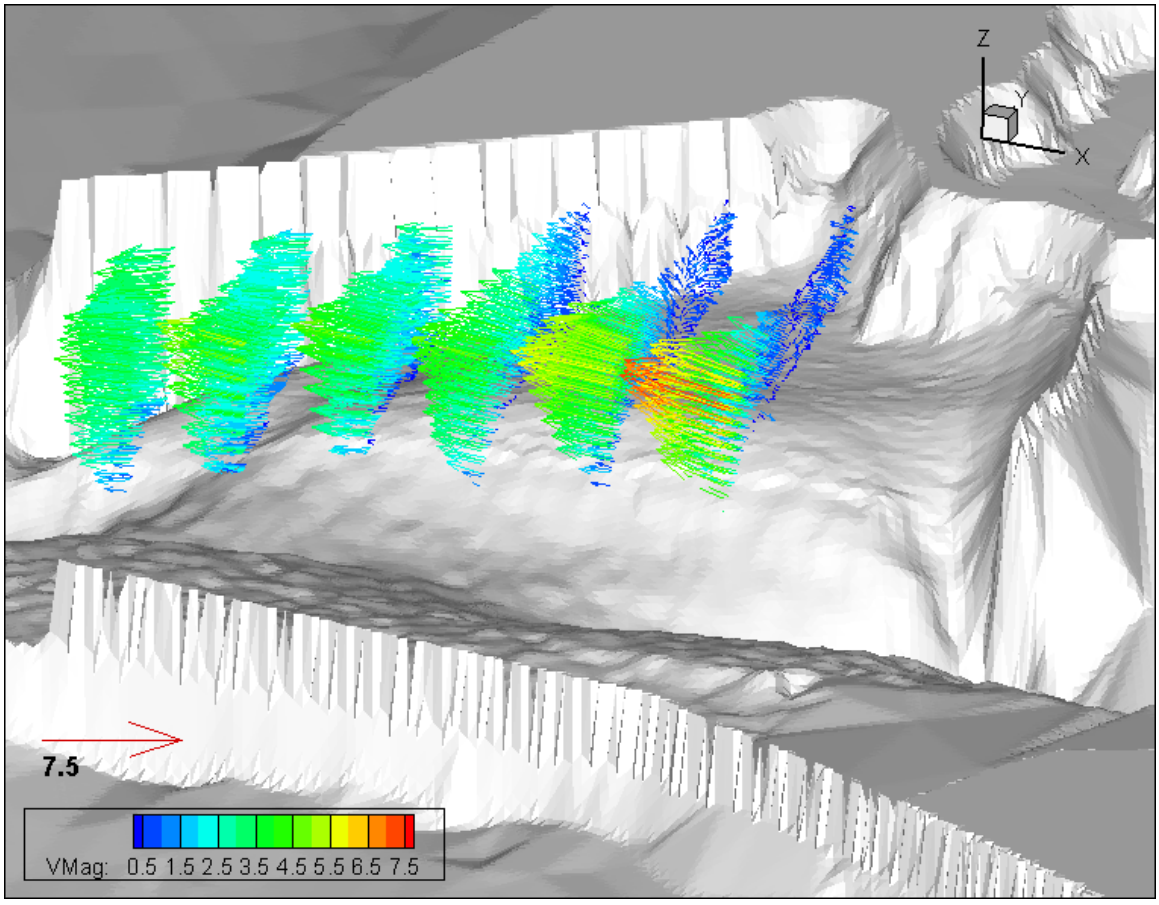

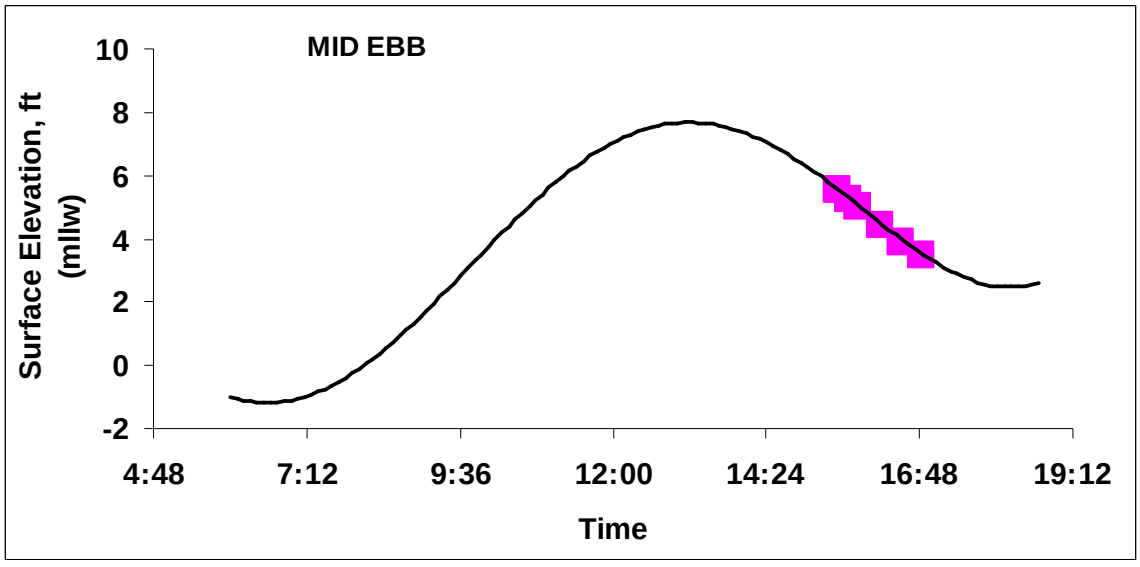

Figure 28 **Three-dimensional projection of the north jetty area with synchronous transects of three-dimensional velocity vectors during peak ebb on 12 August 2003**

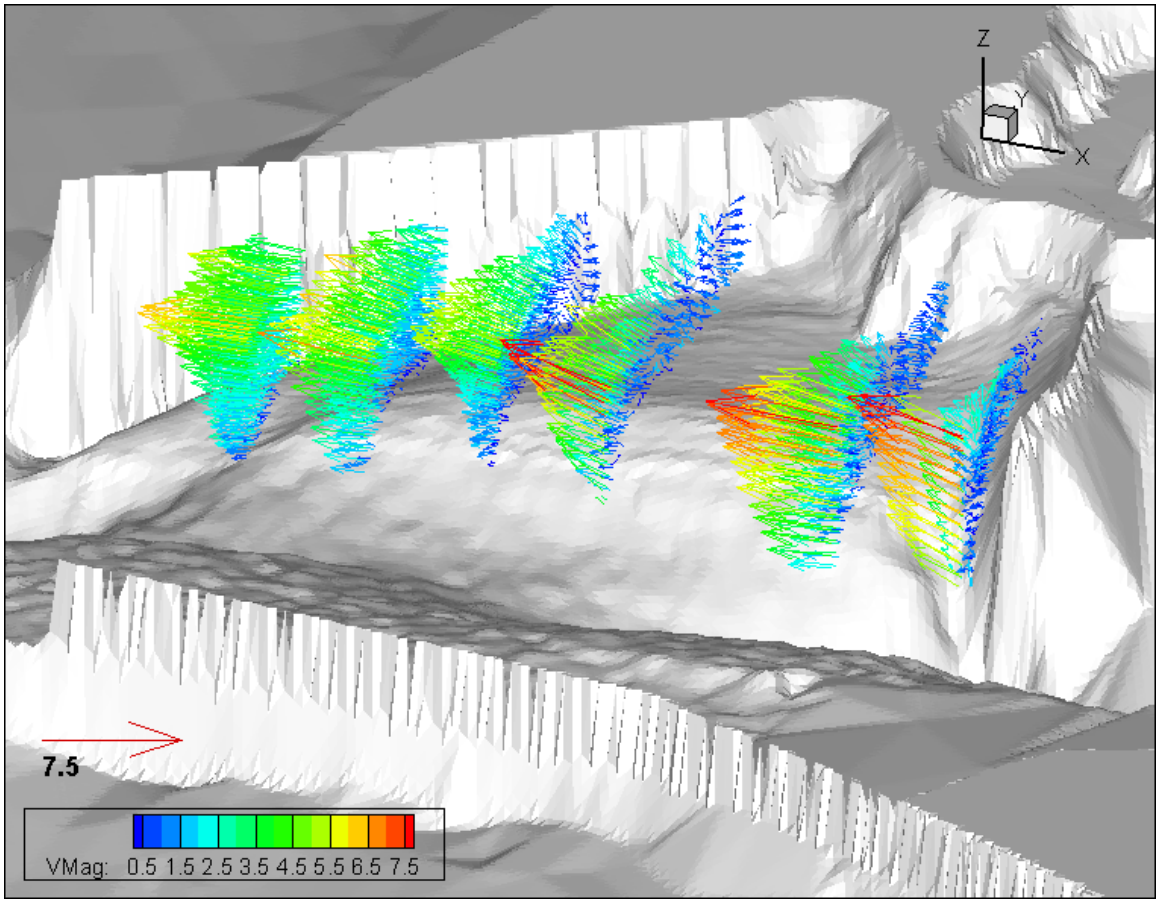

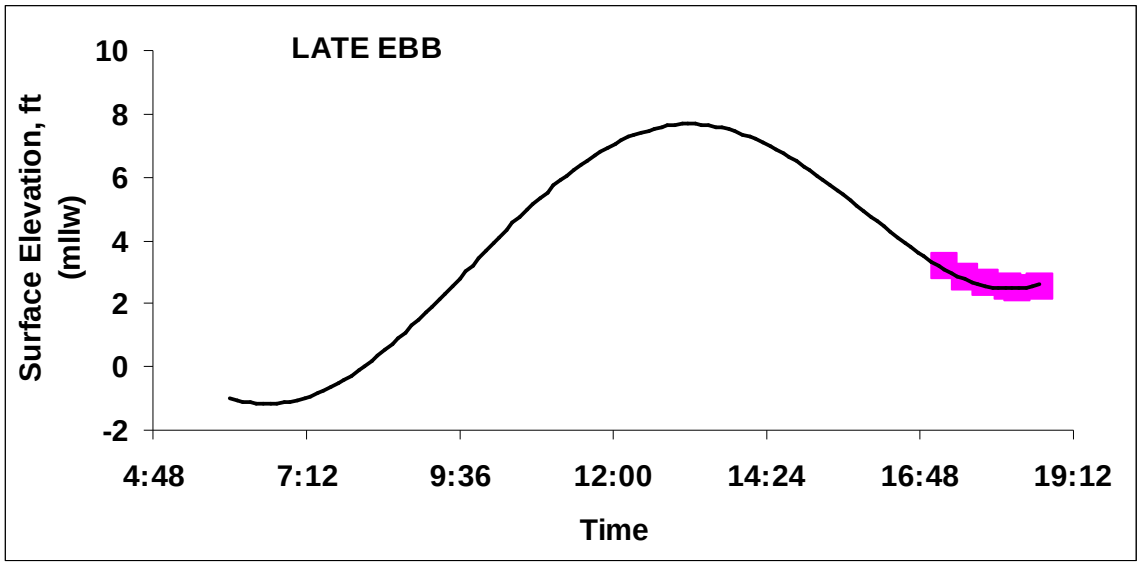

Figure 29 **Three-dimensional projection of the north jetty area with synchronous transects of three-dimensional velocity vectors during late ebb on 12 August 2003**

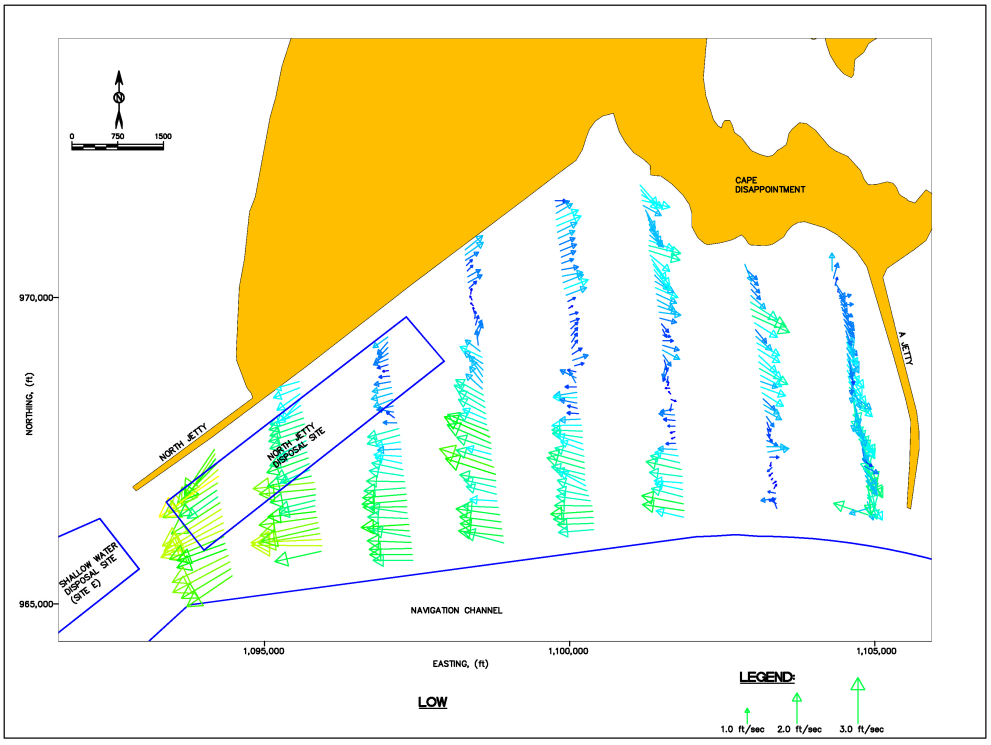

Figure 30 **Depth averaged current vectors along ADP transects at low tide (late ebb) on 13 August 2003**

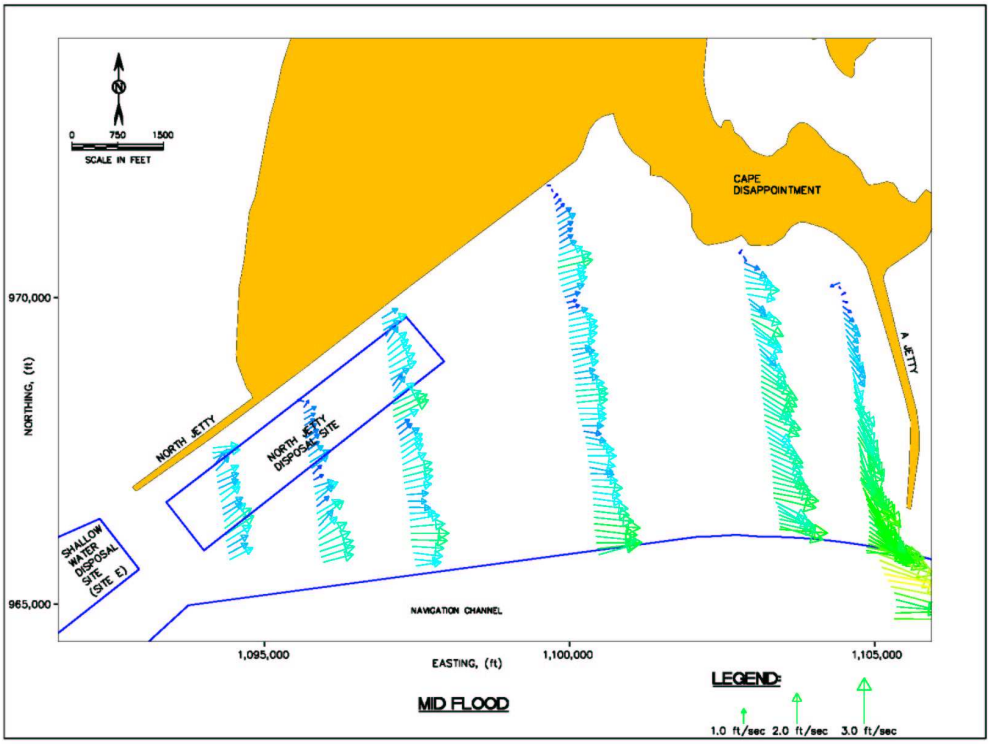

Figure 31 **Depth averaged current vectors along ADP transects during mid flood on 13 August 2003**

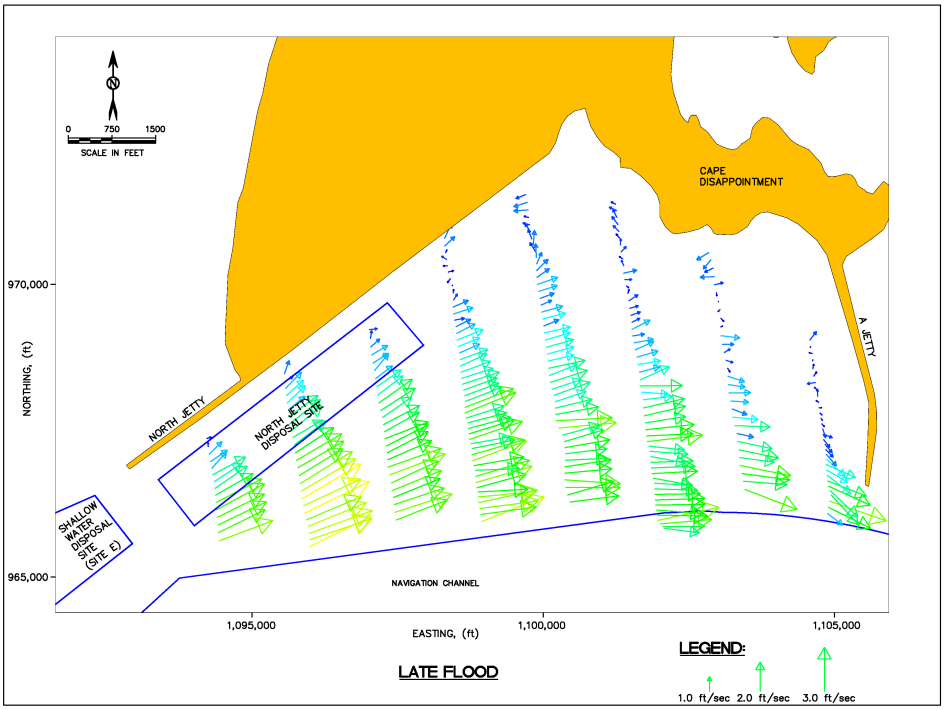

Figure 32 **Depth averaged current vectors along ADP transects during late flood on 13 August 2003**

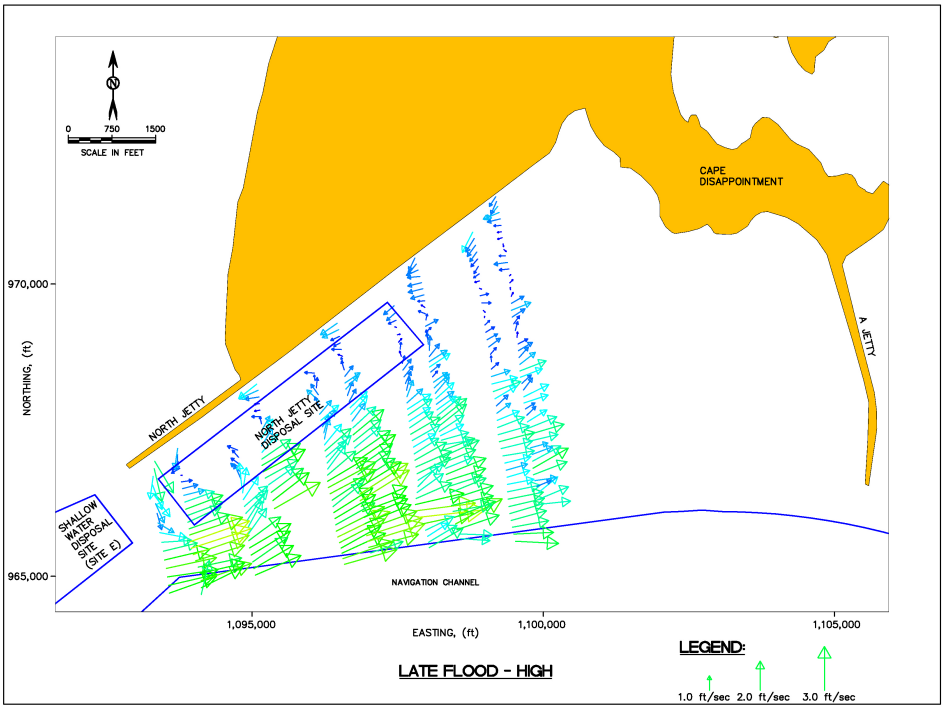

Figure 33 **Depth averaged current vectors along ADP transects during late flood to high tide on 13 August 2003**

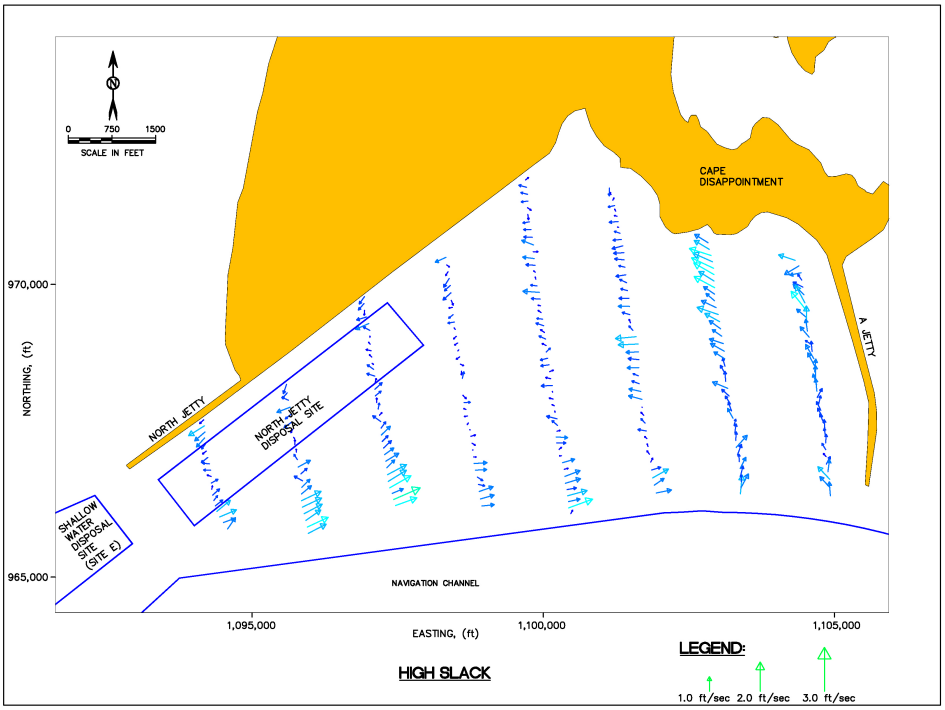

Figure 34 **Depth averaged current vectors along ADP transects during high tide slack on 12 August 2003**

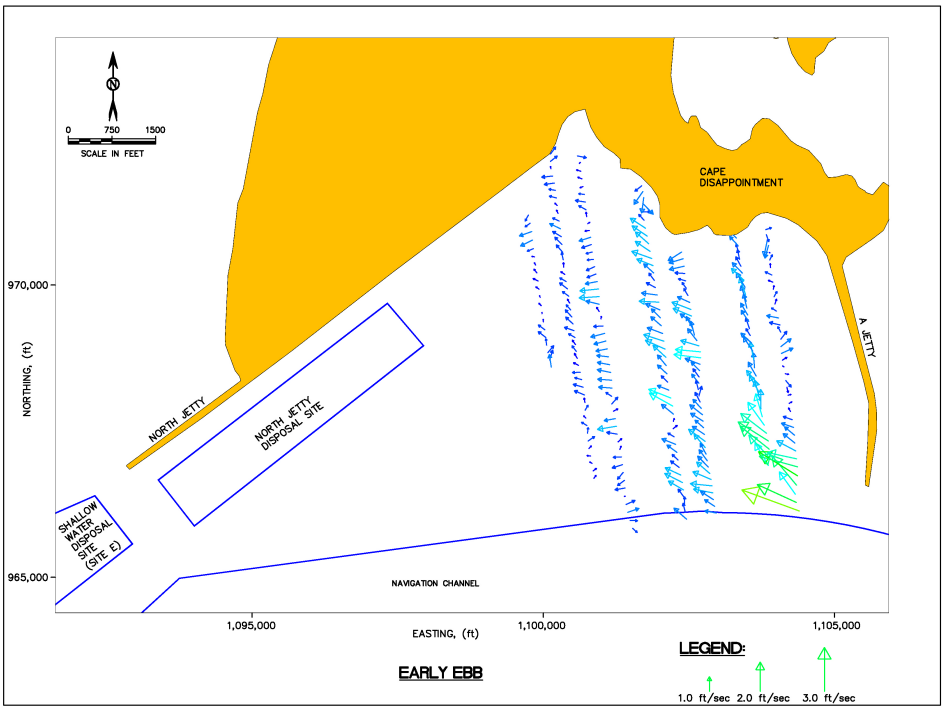

Figure 35 **Depth averaged current vectors along ADP transects during early ebb on 13 August 2003**

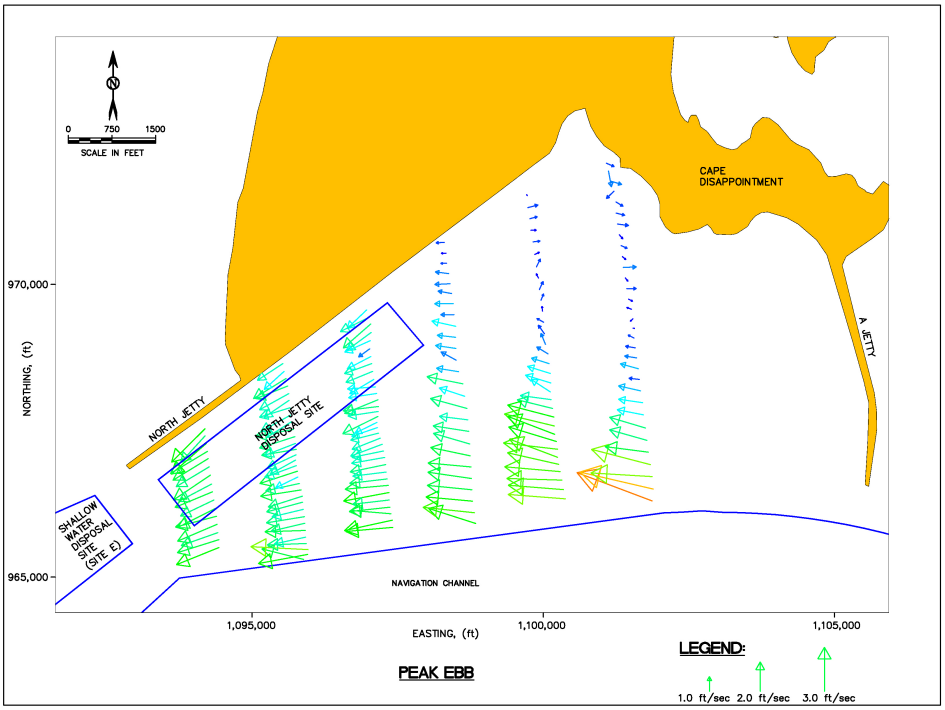

Figure 36 **Depth averaged current vectors along ADP transects during peak ebb on 12 August 2003**

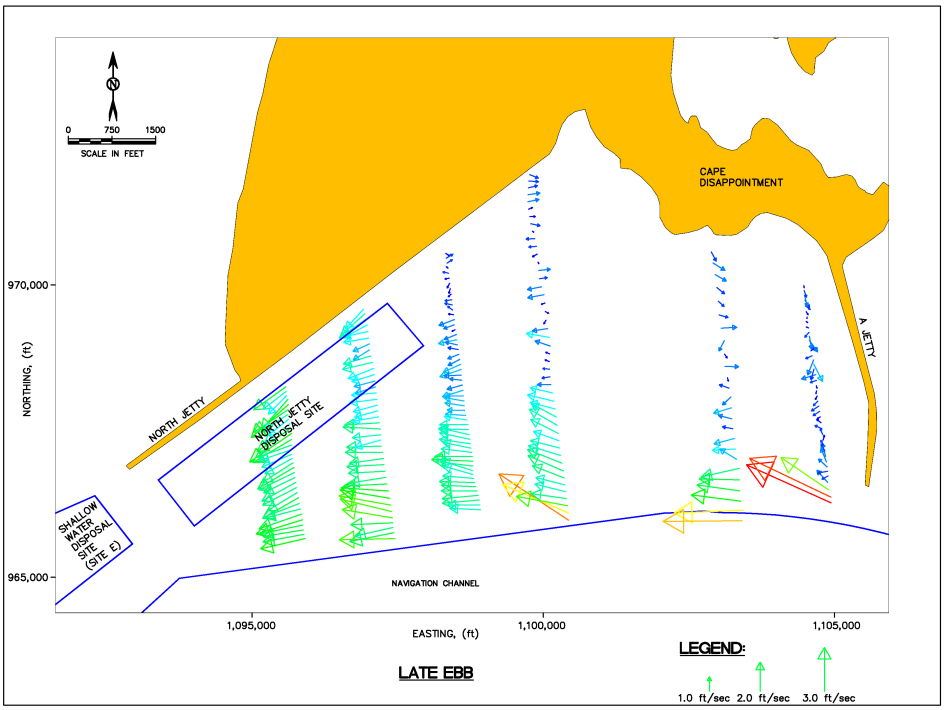

Figure 37 **Depth averaged current vectors along ADP transects during late ebb on 12 August 2003**

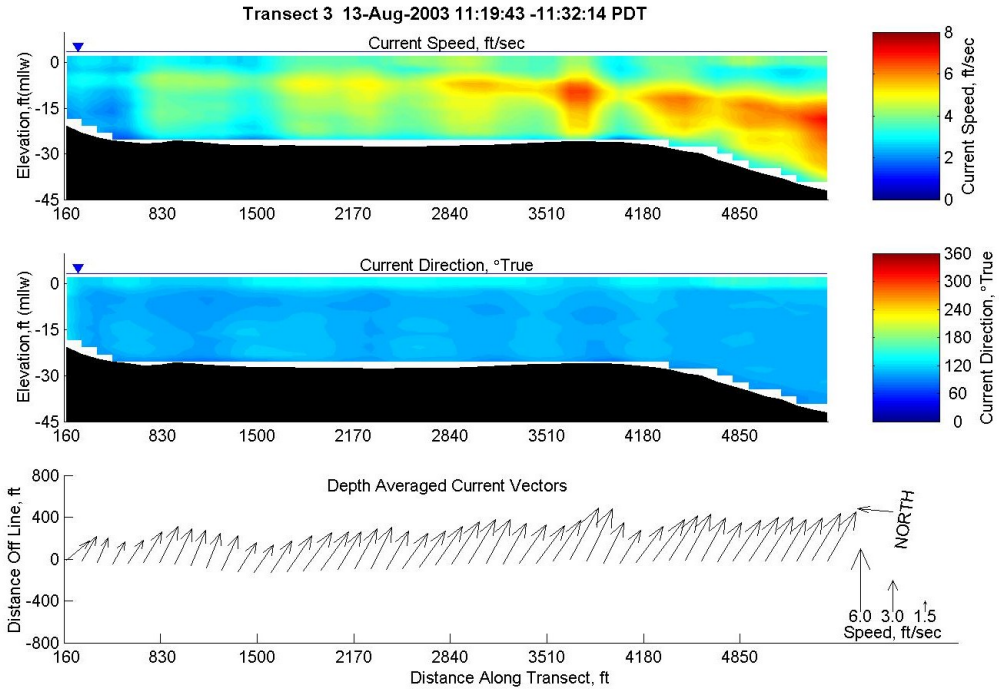

Figure 38 View looking east of current speed and direction profiles along ADP transect 3 between the north jetty and navigation channel on 13 August 2003 during peak flood

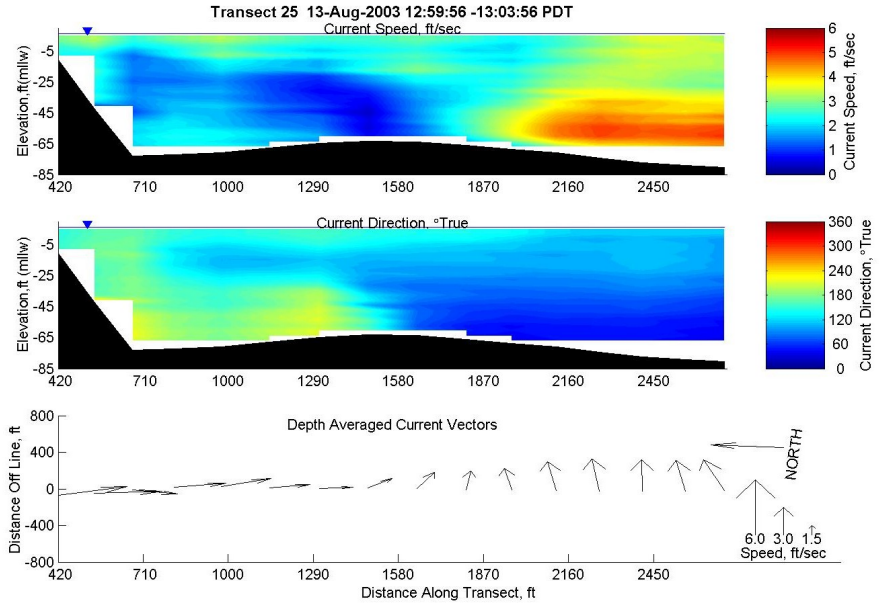

Figure 39 View looking east of current speed and direction profiles along ADP transect 25 between the north jetty and navigation channel on the west end of North Jetty Disposal Site on 13 August 2003 during later flood to high tide.

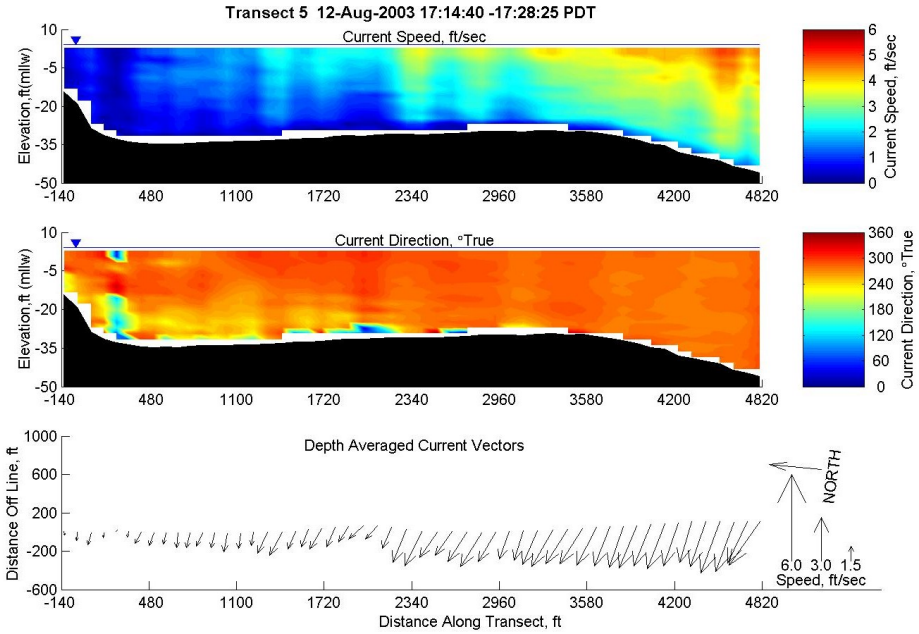

Figure 40 **View looking east of current speed and direction profiles along ADP transect 5 between the north jetty and navigation channel on 12 August 2003 during peak ebb**

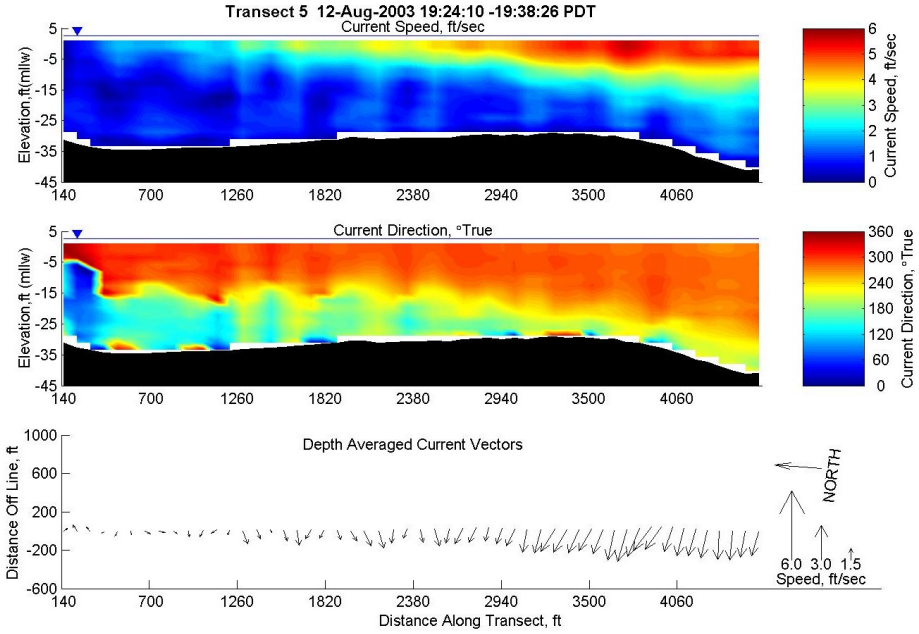

Figure 41 **View looking east of current speed and direction profiles along ADP transect 5 between the north jetty and navigation channel on 12 August 2003 during late ebb**

5. Summary of Main Findings

Field measurements of waves, currents and sediment transport were collected in the area south of north jetty and west of Cape Disappointment at MCR during the summer dredging season in 2003. The measurements were acquired to assist the evaluation of potential constraints and impacts of processes on various dredge and sediment re-handling operations in the area, and the potential for disruption of tidal hydraulics and sediment dynamics, a dredge re-handling operation. The measurements also provide data to verify wave, current, and sediment transport numerical models, thereby advancing their value as tools to aid in evaluation of alternatives.

Analysis of the field measurements collected in 2003 support the following conclusions:

- Offshore H_s during the summer dredging window is less than 1.5 m more than 50 percent of the time.
- The north jetty significantly shelters the area south of north jetty from ocean waves which predominately arrive from north of west during the summer dredging season. H_s has exceeded 1 m less than 5 percent of the time within 500 m south of the north jetty and less than 50 percent of the time within approximately 1500 m of the north jetty in each of the last 3 summer field measurement programs (2000, 2002, and 2003).
- Measurements of H_s, T_p, and *DIR* in the three summer field programs provide a good representation of the wave climate for the project area relative to longer-term measurements for the region.
- During non-storm intervals, H_s in the project area increases during the falling tide (ebb currents and decreasing water depth) reaching a maximum just prior to low tide and decreases on a rising tide (flood currents and increasing depth) reaching a minimum at approximately high tide. Ebb currents and decreasing water depth on a falling tide cause increased wave shoaling while flood currents and increasing depth reduce shoaling on a rising tide.
- Between the north and south jetties, the strength of tidal forcing increases relative to storm- and wave-driven currents, though wave orbital velocities may dominate the near bottom velocity field at most locations in the area south of north jetty, particularly at low water and high water slack.
- Current patterns in the project area are complex with the presence of horizontal eddies (gyres) and evidence of vertical stratification at times during the tidal cycle. However, major features of the circulation are well described by depth-averaging.
- The weakest currents consistently occur in the northeast corner of the project area within 500 to 750 m radius of the eastern terminus of the north jetty and Cape Disappointment. Time- and depth-averaged current speeds rarely exceed 0.5 m/sec in this area. Re-circulation gyres with

opposing spin occur in this area during ebb and flood phases of spring tidal cycles.

- Re-suspension of bottom sediment in the project area is mostly controlled by shear stress induced by wave orbital motions combined with tidal currents near the seabed. Suspended sediment concentrations are generally low (< 1-2 g/l) except when significant swell (H_s >1 m) is present.

6. References

Allan, J. C. and Komar, P. D. 2002. "The wave climate of the eastern North Pacific: Long-term trends and an El Niño/La Niña dependence," Southwest Washington Coastal Erosion Workshop 2000, G. Gelfenbaum, and G. M. Kaminsky (eds.), Open-file-report 02-229.

Earle, M.D., McGehee, D., Tubman, M (1995). "Field wave gaging program, wave data analysis standard," U.S. Army Corps of Engineers, Waterways Experiment Station, Instruction Report CERC-91-1.

Folonoff, N.P. and Millard R.C. Jr. (1983). "Algorithms for computation of fundamental properties of seawater." UNESCO Technical Papers in Marine Science No. 44. Division of Marine Sciences, UNESCO, Paris, France.

McGehee, D.D. and Mayers, C.J. (2000). "Deploying and Recovering Marine Instruments With a Helicopter." Coastal Engineering Technical Note ERDC/CHL CETN-V1-34, U.S. Army Engineer Research and Development Center, Vicksburg, MS.

Moritz, H.R., Moritz, H.P., Hays, J.R., Sumerell, H.R. 2003. 100-years of shoal evolution at the mouth of the Columbia River: impacts on channel, structures, and shorelines. Proceedings of Coastal Sediments 2003, Clearwater Beach, Florida, ASCE, NY (CD-ROM).

Osborne, P.D. 2003. "Oceanographic setting: field measurements and analysis". Chapter 4, in N.C. Kraus, and H.T. Arden, (eds.) North Jetty Study, Grays Harbor, Washington. Volume I: Main Text. ERDC-CHL-TR-03-12.

Pacific International Engineering 2003. "2002 Monitoring Program Report: Benson Beach Demonstration Project Phase 1". Coastal Communities of Southwest Washington, 54p.

APPENDIX A

High resolution three-dimensional projection of digital elevation model (DEM) of the Mount of Columbia River based on bathymetry surveys obtained in 2003

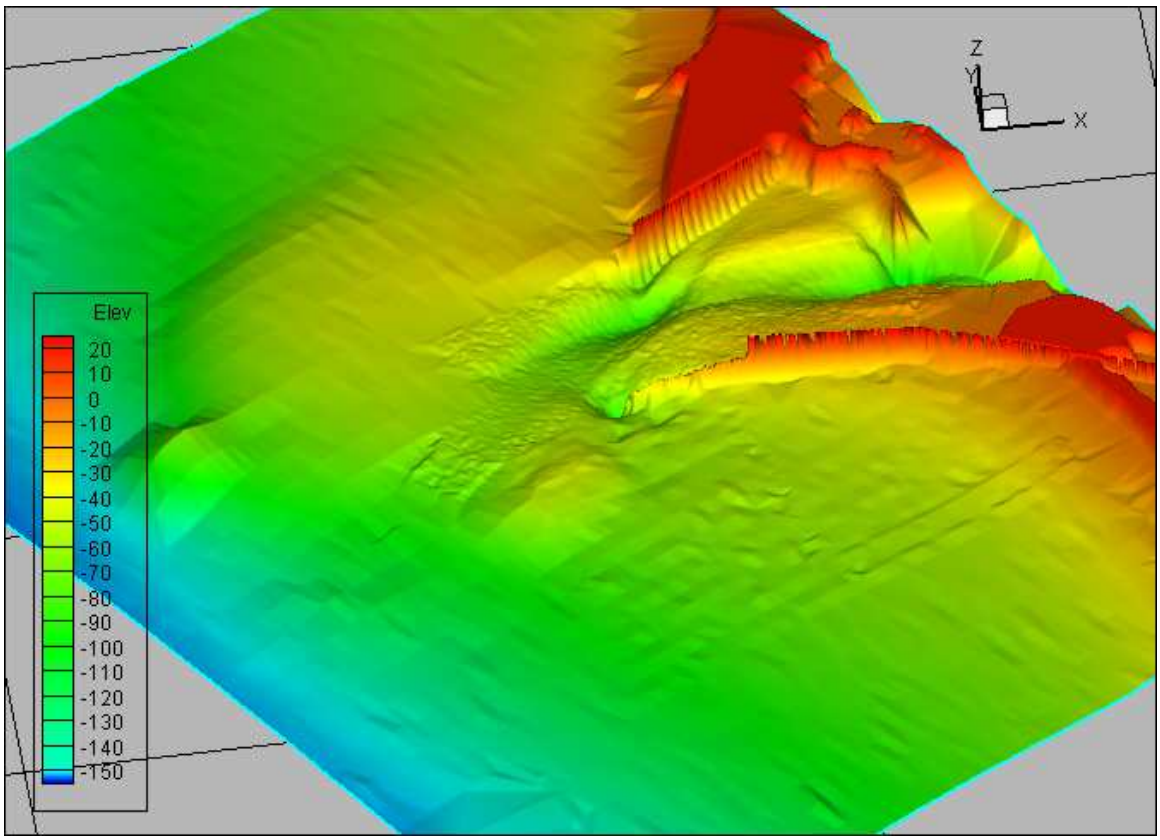

Figure A-1 Three-dimensional projection of digital elevation model for the Mouth of Columbia River constructed from a 100-ft rectilinear grid

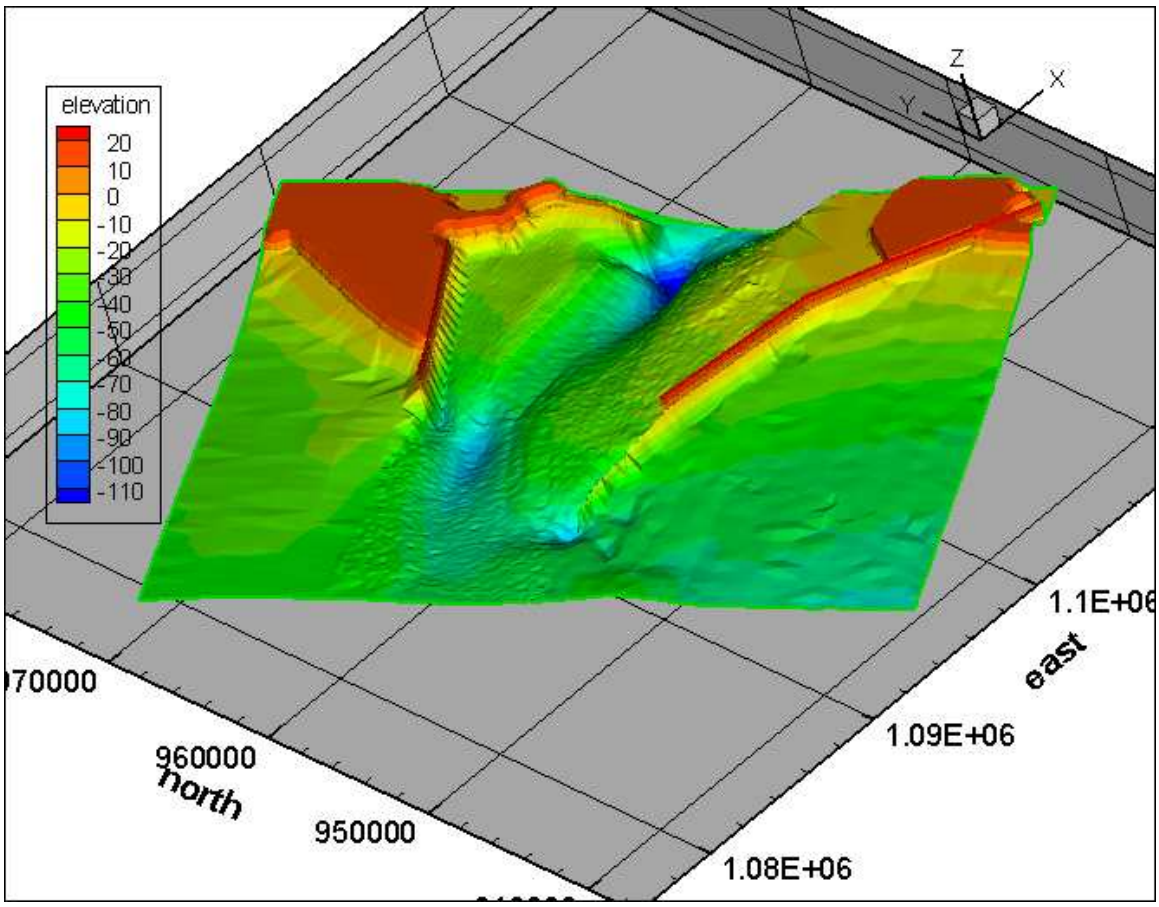

Figure A-2 Three-dimensional projection of digital elevation model for the Mouth of Columbia River constructed from a 25-ft rectilinear grid

APPENDIX B

ADP Transect Cross-sections